ARTICLE

OBC
www.rsc.org/obc

Design, synthesis, conformational analysis and nucleic acid hybridisation properties of thymidyl pyrrolidine-amide oligonucleotide mimics (POM)†

David T. Hickman,[a] T. H. Samuel Tan,[a] Jordi Morral,[a] Paul M. King,[b] Matthew A. Cooper[c] and Jason Micklefield*[a]

[a] *Department of Chemistry, University of Manchester Institute of Science and Technology, Faraday Building, PO Box 88, Manchester, UK M60 1QD*

[b] *Department of Chemistry, Birkbeck College, University of London, 29 Gordon Square, London, UK WC1H 0PP*

[c] *University Chemical Laboratory, Lensfield Road, Cambridge, UK CB2 1EW*

Received 30th May 2003, Accepted 6th August 2003
First published as an Advance Article on the web 28th August 2003

Pyrrolidine-amide oligonucleotide mimics (POM) **1** were designed to be stereochemically and conformationally similar to natural nucleic acids, but with an oppositely charged, cationic backbone. Molecular modelling reveals that the lowest energy conformation of a thymidyl-POM monomer is similar to the conformation adopted by ribonucleosides. An efficient solution phase synthesis of the thymidyl POM oligomers has been developed, using both *N*-alkylation and acylation coupling strategies. ^{1}H NMR spectroscopy confirmed that the highly water soluble thymidyl-dimer, T_2-POM, preferentially adopts both a configuration about the pyrrolidine *N*-atom and an overall conformation in D_2O that are very similar to a typical C3′-*endo* nucleotide in RNA. In addition the nucleic acid hybridisation properties of a thymidyl-pentamer, T_5-POM, with an *N*-terminal phthalimide group were evaluated using both UV spectroscopy and surface plasmon resonance (SPR). It was found that T_5-POM exhibits very high affinity for complementary ssDNA and RNA, similar to that of a T_5-PNA oligomer. SPR experiments also showed that T_5-POM binds with high sequence fidelity to ssDNA under near physiological conditions. In addition, it was found possible to attenuate the binding affinity of T_5-POM to ssDNA and RNA by varying both the ionic strength and pH. However, the most striking feature exhibited by T_5-POM is an unprecedented kinetic binding selectivity for ssRNA over DNA.

Introduction

Modified nucleic acids and oligonucleotide mimics are of considerable interest as agents for down-regulating gene expression through hybridisation either with target mRNA (antisense) or dsDNA (antigene).[1–6] This approach has not only led to new therapeutic treatments, but is widely used in target validation to identify new therapeutic targets. In addition, modified oligonucleotides are of value as diagnostic and bio-analytical probes, or as tools in molecular biology.[6–11] These molecules are also of fundamental importance as models to explore the structure–function relationship of nucleic acids.[12,13] In particular, by studying the biophysical properties of chemically modified nucleic acids, it is argued that we can gain insight as to why DNA and RNA were selected as the ubiquitous genetic materials on this planet.[14]

Despite the large number of backbone modifications that have been developed, surprisingly few confer enhanced recognition properties, affinity and sequence selectivity, for DNA and RNA relative to native nucleic acids.[1,15] A general strategy to enhance affinity has been to develop modified oligonucleotides that are better pre-organised by restricting the conformational freedom of the backbone.[1,16] For example, sugar modifications which retain the native phosphodiester linkage, such as LNA **2** (Fig. 1),[17,18] have been used to particularly good effect.[5,6,11] Several groups have also replaced the phosphodiester linkage in nucleic acids with alternative neutral linkages based on the premise of favourable enthalpy changes resulting from diminished electrostatic repulsion between strands.[1] However even

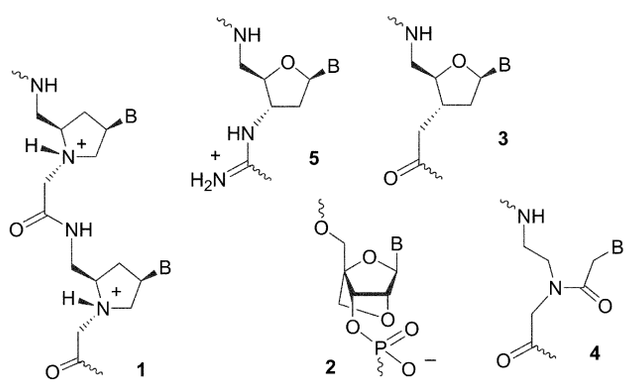

Fig. 1 Structure of POM and other related oligonucleotide mimics. B = nucleobase (A, T, C or G).

the best of all neutral linkages, for example amide **3**[19] or 3′-*N*-sulfamate modified DNA,[20] result in only modest increases in affinity for complementary nucleic acids. Of all the neutral mimics that have been developed, probably PNA **4**, where the whole backbone is replaced by a pseudo peptide structure,[21–23] is the most effective and widely used.[7–10] Nevertheless PNA suffers from poor aqueous solubility and a tendency to aggregate. In addition PNA is achiral and can bind in both a parallel and antiparallel fashion with nucleic acid, which can jeopardise sequence specificity.

The introduction of positive charges into the backbone of oligonucleotide mimics is an alternative approach for increasing the affinity for complementary DNA and RNA. One of the earliest examples reported was the deoxynucleic guanidine (DNG) **5** oligomers, where the phosphodiester linkages in DNA are replaced by cationic guanidinium groups.[24] This

† Electronic supplementary information (ESI) available: experimental details (16 Figures, 3 Tables). See http://www.rsc.org/suppdata/ob/b3/b306156f/

DOI: 10.1039/b306156f

modification was shown to vastly increase affinity for complementary ssDNA and RNA. However, it remains to be seen if such strong electrostatic attraction between oppositely charged backbones results in non-specific binding, *via* salt bridges, which may not necessitate base pairing and therefore may not be evident from standard UV thermal denaturation experiments.

As part of current research in our laboratory into the development of backbone modified oligonucleotides, we recently introduced the novel cationic pyrrolidine-amide oligonucleotide mimic (POM).[25] In this paper we describe the design rationale, solution phase synthesis and conformational analysis of thymidyl T_2-POM. Finally, the nucleic acid hybridisation properties of a phthalimide capped T_5-POM are discussed in detail.

Results and discussion

Design and molecular modelling

Pyrrolidine-amide Oligonucleotide Mimics (POM) **1** (Fig. 1) are derived by replacing the furanose ring and phosphodiester backbone in DNA with a (2*R*,4*R*)-configured pyrrolidine ring and amide linkage, respectively. The pyrrolidine ring was chosen because it will be substantially protonated at physiological pH. Due to nearest neighbour interactions[26,27] it is anticipated that only every other pyrrolidine would be protonated at physiological pH. Nevertheless oligomers will possess high water solubility and exhibit electrostatic attraction for complementary nucleic acids, possibly increasing affinity. In this respect it is similar to DNG **5**.[24] It was also envisaged that the binding affinity to DNA/RNA might be attenuated by changing the ionic strength or pH, which may be an attractive property if these molecules are to be used as probes, for example in DNA-microarray type devices. In addition there is some evidence to suggest that positively charged peptides and peptidomimetics (like POM) could bind through electrostatic attraction to phosphate groups of the cell wall, which can aid transport through the cell membranes.[28] The amide linkage was selected to connect the pyrrolidine units, since this group has been shown to be a viable replacement for phosphodiester in the amide-linked DNA mimics.[19] Furthermore the amide linkage should facilitate the synthesis of POM using peptide chemistry and also allow easy conjugation with peptides, in a similar fashion to PNA.

The (2*R*,4*R*) stereochemistry of the pyrrolidine ring was carefully selected because this should ensure that the *N*-acetamido group will adopt the sterically less demanding *trans* relative configuration making the system a stereochemical match with native nucleic acids. Of course the pyrrolidine *N*-atom can invert configuration *via* the free amine at a rate that will depend on pH. However, X-ray crystallographic data[29] for a protonated pyrrolidine ring **6**, which is stereochemically identical and both electronically and sterically similar to the pyrrolidine ring in POM, clearly show that the *N*-alkyl substituent adopts the *trans* relative stereochemistry, at least in the crystalline state (Fig. 2). In addition the overall conformation of **6**, which is described by a pseudorotation phase angle (P)[30,31] of 43.7° and a maximum torsional angle (v_{max}) of 40.7°, is similar to uridine **7** in the crystalline state ($P = 14°$ and $v_{max} = 42°$).[32] In fact pyrrolidine **6** is only a few degrees of pseudorotation out from the preferred C3′-*endo* conformation of ribose in RNA which typically falls within the range $P = 0 \longrightarrow 36°$.[31] As such it was envisaged that the pyrrolidine unit of POM would bear a closer conformational resemblance to native RNA and more conservative mimics such as amide linked DNA **3** and LNA **2** which similarly adopt a C3′-*endo* sugar-conformation. As a result of these critical stereochemical and conformational features POM is predicted to bind in an antiparallel fashion and differs conceptually from other oligonucleotide systems incorporating pyrrolidine units.[33–40] These systems were designed as conformationally restricted analogues of PNA, unlike POM which we envisage shares little conformational or electrostatic similarity with PNA.

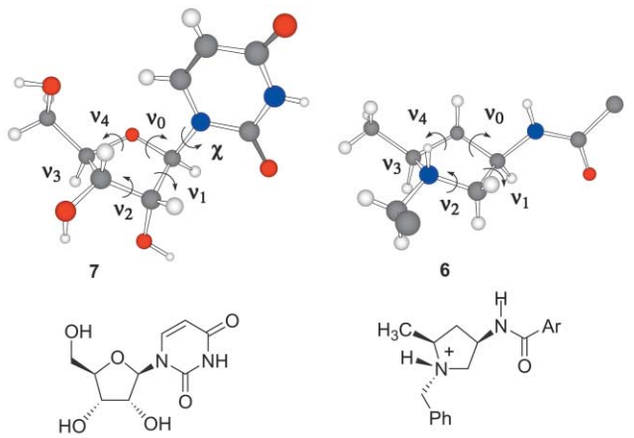

Fig. 2 X-ray crystal structures of pyrrolidine derivative **6**[29] and uridine **7**.[32]

In order to determine the relative energies of the different configurations and conformations of the pyrrolidine ring in POM, semi-empirical quantum mechanical calculations[41] were performed on the model thymidyl-pyrrolidine *cis*- and *trans*-dimethyl diastereoisomers **8** and **9** (Fig. 3). Each conformer, generated for every 10 degrees of pseudorotation, was first energy minimised allowing free rotation of the thymine base about the C4′-N1 bond in order to optimise the pseudo-glycosidic torsion angle (χ). The standard enthalpies of formation for each conformer were then calculated [see Fig. 3 and ESI Table 1]. These reveal that, as predicted, the conformers generated for the *trans*-diastereoisomer **9** are on the whole lower in energy than the *cis*. Moreover the lowest energy *trans*-conformer **A** has a phase angle of 48° which is similar to the crystal structure of pyrrolidine **6** and also just outside that region of conformational space occupied by C3′-*endo* ribose typical for RNA.[31] The *trans*-conformer **B** (P = 198°) is 0.57 kcal mol^{-1} higher in energy and analogous to a C2′-*endo* deoxyribose typically highly populated in DNA structures.

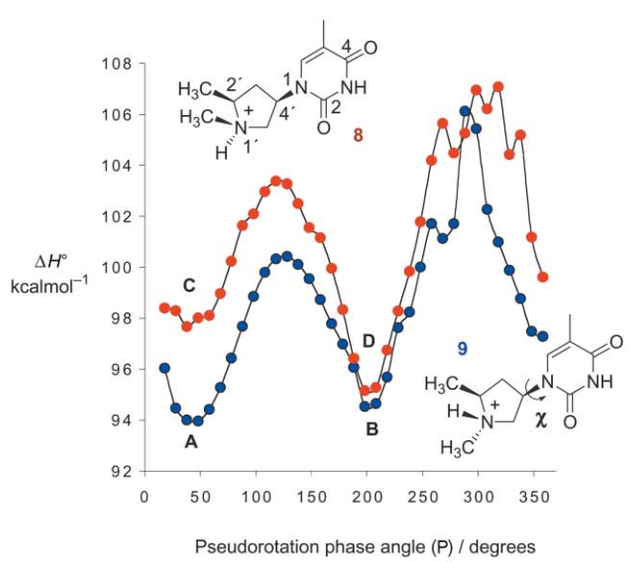

Fig. 3 Variation in the standard enthalpies of formation ($\Delta H°$) with pseudorotation phase angles (P) for model *cis*- and *trans*-dimethyl pyrrolidines **8** and **9**.

Whilst these findings are encouraging and suggest the most highly populated configuration and conformation will match closely the RNA ribose structure, it should be noted these

studies do not account for intramolecular forces that may arise in longer oligomers. For example, one could envisage a possible H-bond extending from the protonated pyrrolidine *N*-atom to an adjacent O-atom of the amide linkage in oligomeric POM **1**. Nevertheless intrastrand electrostatic repulsion should favour the formation of an extended linear structure, with *trans*-relative stereochemistry, and disfavour the formation of tightly folded secondary structures, which might jeopardise base pairing with complementary DNA and RNA.

Synthesis of a thymidyl-POM dimer

In order to investigate the conformational properties of POM, using ^{1}H NMR spectroscopy, the synthesis of a thymidyl-dimer, T_2-POM, was embarked upon first. Accordingly the ester **10** (Scheme 1) was prepared from *trans*-4-hydroxy-L-proline[42] and further transformed to the thymidyl-pyrrolidine **11** in an analogous fashion to the corresponding methyl ester, which was prepared earlier.[33] Reduction of the ester **11** proceeded in 69% yield with concomitant cleavage of the benzoyl-protecting group to give the alcohol **12**. Whilst the cleavage of the benzoyl group was unexpected, it was nevertheless advantageous since thymine-N3 protection was employed to ensure regioselectivity in the previous Mitsunobu reaction,[33] and was not envisaged to be necessary for subsequent transformations. Initially we sought to change the alcohol **12** to the corresponding amine **14** *via* the tosylate **15** and the azide **16**. The tosylate **15** was thus prepared in essentially quantitative yield, but upon heating to 80 °C with LiN_3 in DMF for 16 h surprisingly none of the expected azide **16** was obtained. Instead the 6-enamine-bridged tricyclic compound **18** was isolated as the major product. Presumably under the thermal conditions of substitution reaction the azide **16** undergoes an intramolecular 1,3-dipolar cycloaddition with the C5–C6 double bond of the thymine ring.[43,44] The resulting fused triazoline **17** presumably spontaneously rearranges to give **18**. In order to circumvent this, the alcohol **12** was converted into the corresponding phthalimide derivative **13** under standard Mitsunobu conditions. Removal of the phthaloyl group from **13** proceeded in 92% yield on treatment with 40% aqueous methylamine, at 40 °C for 1 h, to furnish amine **14**.

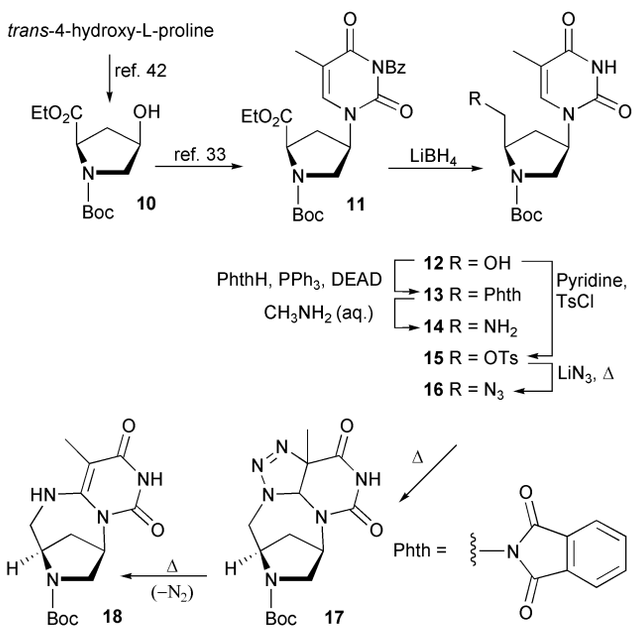

Scheme 1

Two different approaches were envisaged for chain extension of POM. In the first approach *N*-alkylation of the pyrrolidine **19** with bromoacetamide **20** was investigated (Scheme 2).

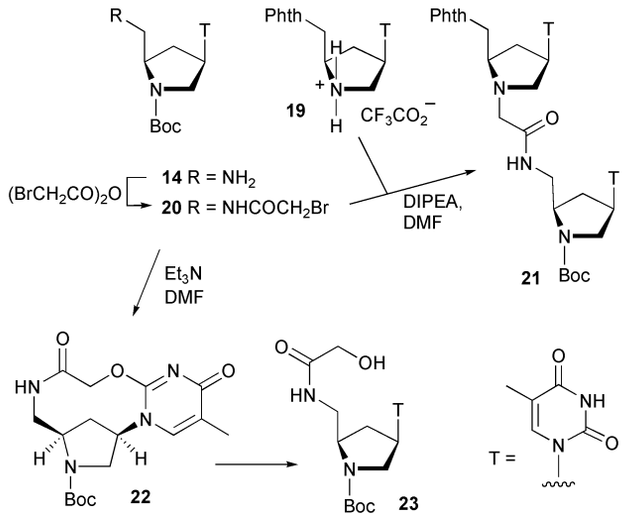

Scheme 2

Accordingly a solution of the primary amine **14** in dry dichloromethane was added slowly to a 65% (w/v) solution of bromoacetic anhydride in acetonitrile at −15 °C, which resulted in a near quantitative yield of the bromoacetamide **20**. Removal of the Boc protecting group from **13** under standard conditions gave the secondary amine **19** as the TFA salt in essentially quantitative yield. Coupling bromoacetamide **20** with this amine salt **19** in the presence of Et_3N and DMF, however, gave the dinucleotide analogue **21** in a disappointingly low 58% yield. A major side product from this reaction was the primary alcohol **23**. However, when this coupling was attempted using DIPEA instead of Et_3N, the yield of dimer **21** rose dramatically to 98% with no observed side products. In both cases the reactions were carried out under totally anhydrous conditions. It seems most plausible that the less sterically hindered base triethylamine can deprotonate the acidic proton on thymine (N3H pK_a = 9.7)[31] to liberate a nucleophilic neighbouring group, which could participate in an intramolecular S_N2 displacement of the bromide to give the lactam **22**. This intermediate **22** could not be isolated probably because it undergoes facile hydrolysis, either on TLC or during the aqueous workup, to give the side-product **23**.

Whilst the *N*-alkylation approach (**19** + **20** ⟶ **21**) using DIPEA in DMF was excellent in terms of yield, the reaction proceeded slowly at room temperature (18 h) and would therefore not be ideal for future application in the solid-phase synthesis of POM. Dimer formation using an acylation approach was therefore also investigated (Scheme 3). Thus amine **19** was treated with *tert*-butyl bromoacetate to give the ester **24**, which upon treatment with 20% TFA in dichloromethane gave acid **25** as a TFA salt. This acid **25** was then transformed into the pentafluorophenyl ester **26** in 85% yield using pentafluorophenyl trifluoroacetate. Acylation of primary amine **14** with the Pfp-ester **26** proceeded smoothly at room temperature in dichloromethane and after 3 h gave the protected dinucleotide analogue **21** in quantitative yield.

In order to obtain the fully deprotected T_2-POM **30** for NMR-conformational studies, dinucleotide mimic **21** was treated with methylamine, as before, in order to remove the phthaloyl protecting group. However, three products were isolated: the desired amine-dimer **27** as well as bicyclic lactam **28** and the amine-monomer **14**. Clearly the basic conditions required for removal of the phthaloyl group facilitate cyclisation *via* the attack of the *N*-terminal amine on the central amide linkage. This problem was overcome, to an extent, by lowering the reaction temperature to room temperature and stopping the reaction after only 40 min. This led to a mixture of the desired product **27** and an intermediate, presumably the ring-opened phthaloyl derivative **29**. The latter was separated

Table 1 ^{1}H NMR conformational analysis of T_2-POM·3HCl **30**

Vicinal H–H	Observed $^3J_{HH}$/Hz for **30**[a]	Calculated $^3J_{HH}$/Hz[b] (dihedral angle ϕ_{HH}/deg)[c] for conformer			Karplus parameters [r][d]		
		A $P = 48°$	**C** $P = 38°$	**B** and **D** $P = 198°$	a_j	b_j	c_j
2′–3′	9.9[a]	10.2[b] (157)[c]	10.0 (155)	1.3 (92)	9.6	−0.99	1.2
2′–3″	7.4	5.8 (42)	5.9 (41)	8.4 (23)	9.6	−0.99	1.2
3′–4′	6.2	8.0 (143)	6.7 (136)	2.9 (113)	9.7	−0.99	1.0
3″–4′	9.6	8.2 (25)	8.7 (20)	9.8 (2)	9.7	−0.99	1.1
4′–5′	3.7	3.4 (117)	2.5 (110)	7.3 (140)	9.2	−0.99	1.1
4′–5″	8.8	9.0 (1)	8.9 (7)	8.1 (20)	8.6	−0.99	1.4

[a] The observed $^3J_{HH}$ coupling constants for the tri-substituted "upper" pyrrolidine ring of T_2-POM·3HCl **30**. [b] The calculated $^3J_{HH}$ coupling constants and [c] dihedral angles for the vicinal protons of the lowest energy conformers **A–D** of the model *cis*- and *trans*-dimethyl pyrrolidines **8** and **9** (Fig. 3). [d] The Karplus parameters a_j, b_j and c_j derived previously for L-4-hydroxyproline[45] were used in the generalised Karplus equation to calculate $^3J_{HH}$ (see Experimental section).

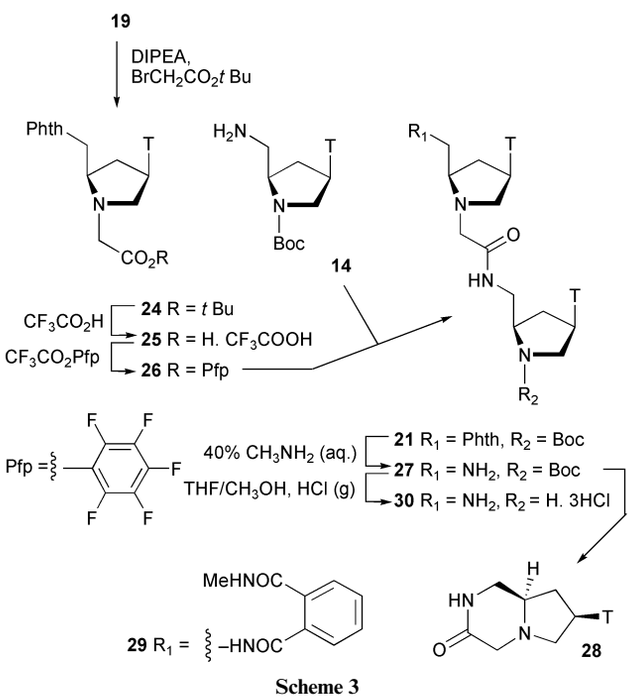

Scheme 3

and then treated with more methylamine to give amine **27** in a combined yield of 75%. Treatment of the amine **27** with HCl gave the totally deprotected hydrochloride salt T_2-POM **30** that was used in the following conformational studies.

NMR conformational analysis of T_2-POM

In order to analyse the conformation of POM in aqueous solution, the tri-cationic T_2-POM **30** was subjected to extensive 2D ^{1}H NMR analysis. The ^{1}H NMR spectrum of **30**, in D_2O, was fully assigned with the aid of COSY-45, TOCSY, ROESY and *J*-resolved experiments. Vicinal coupling constants were obtained for every proton on the trisubstituted "upper" pyrrolidine ring and these are shown in Table 1. Theoretical coupling constants were also calculated, using a generalised Karplus equation,[45] and the dihedral angles obtained for the four lowest energy conformers **A**, **B**, **C** and **D**, that were derived previously from calculations performed on the model *cis*- and *trans*-diastereoisomers **8** and **9** (Fig. 3). The experimentally observed ^3J values from T_2-POM **30** were then compared with the calculated $^3J_{HH}$ values of the model conformers (Table 1). Noticeably the H2′–H3′ coupling constant ($^3J_{2'3'}$) of 9.9 Hz observed for the upper ring of dimer **30** (Fig. 4) corresponds well to the calculated values for both conformers **A** and **C** where the H2′–H3′ dihedral angles ($\phi_{2'3'}$) are 157° and 155° respectively. In contrast both conformers **B** and **D** have identical pucker (P = 198°) and thus equivalent dihedral angles ($\phi_{2'3'}$ = 92°), which correspond to a typically small calculated $^3J_{2'3'}$ of 1.3 Hz. Similarly, the observed $^3J_{3'4'}$ and $^3J_{4'5'}$ coupling constants of 6.2 and 3.7 Hz correspond more closely with the calculated values for either structure **A** or **C**. Thus, the observed ^3J values are in best overall agreement with the structures **A** (P = 48°) or **C** (P = 38°), both of which are analogous to the northern or C3′-*endo* ribose ring conformations.

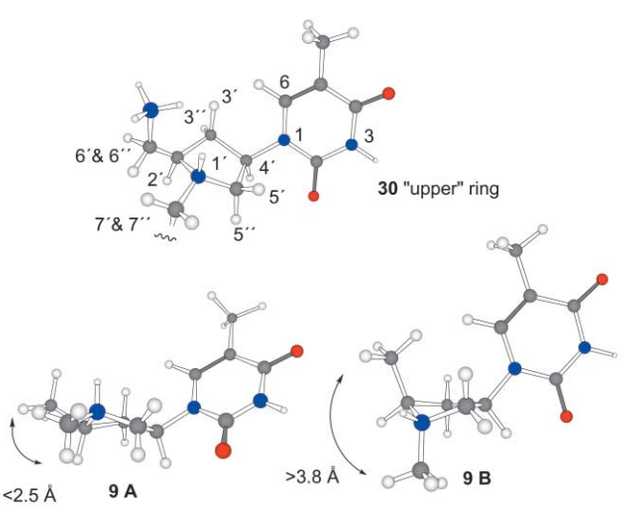

Fig. 4 Numbering system for the tri-substituted "upper" pyrrolidine ring of T_2-POM·3HCl **30** and 3D structures of the lowest energy conformers **A** and **B** of *trans*-dimethyl pyrrolidine **9** from Fig. 3.

The analysis of ^3J values provides no information regarding the preferred configuration of the pyrrolidine *N*-atom. In this respect through space H–H correlations, as determined by ROESY spectra, proved most useful. Notably H7′/7″–H2′ and H7′/7″–H5″ ROE cross-peaks are observed for **30** (Fig. 4) whereas no cross-peaks exist between H7′/7″ and H5′ or H3′. This is most consistent with the *trans N*-configuration of conformers **A** and **B** where the distances between H7′/7″ and H2′ or H5″ are in the order of 2.5 Å. In addition, H7′/7″–H6′/6″ cross-peaks are evident. This is most consistent with conformer **A**,

where the C7′–C6′ dihedral angle is 76° which places the corresponding protons within 2.5 Å. However, in conformer **B**, the corresponding dihedral angle is much larger, 155°, which places these protons more than 3.8 Å apart (Fig. 4). Interestingly, H6–H3′ and H6–H5′ cross-peaks are also detected as well as a H6–H4′ cross-peak, which suggests that the thymine ring is in equilibrium between the *anti* and *syn* conformations, relative to the pyrrolidine ring. A similar conformational equilibrium is often observed with natural nucleosides.[31] In summary both observed $^3J_{HH}$ coupling constants and ROEs for the tri-substituted "upper" pyrrolidine ring in **30** are consistent with the conformer **A** (Fig. 4). This configuration and conformation was also the lowest energy structure determined by modelling. Whilst it is possible that the tri-substituted pyrrolidine ring in **30** is in equilibrium between several conformations, in solution, the fact that the NMR and modelling studies are consistent suggests that the most highly populated, lowest energy structure is that which most closely matches a typical nucleotide in RNA.

Synthesis of T_5-POM

For our preliminary investigations into the nucleic acid hybridisation properties of POM we decided to synthesise and evaluate T_5-POM. The synthesis toward T_5-POM proceeded using iterative alkylation of the pyrrolidine ring with the bromoacetamide **20** already in hand. Accordingly, Boc protected T_2-POM **21** was treated with trifluoroacetic acid to give the secondary amine **31**, as the TFA salt. Coupling of **31** with bromoacetamide **20** proceeds in DMF with excess DIPEA to give Boc protected T_3-POM **32**, in near quantitative yield (Scheme 4). Repeating this Boc deprotection/coupling cycle leads to the Boc protected T_4- and T_5-POM **33** and **34** respectively, in similarly satisfactory yields after purification by silica gel chromatography. Complete assignment of the ^{1}H and ^{13}C NMR spectra of these protected oligomers **32**–**34** was significantly complicated due to spectral overlap. Nevertheless the signals of the thymine CH_3 and C4 carbon atoms are clearly resolved in the ^{13}C NMR spectra recorded in CD_3OD (see ESI Fig. 2), whilst the thymine NH signals can be distinguished from the ^{1}H NMR in DMSO-d_6 (see ESI Fig. 3). Attempts to remove the phthaloyl group of Phth-T_5-Boc POM **34**, again using aqueous methylamine, proved unsuccessful and were ultimately abandoned. It appears that base catalysed decomposition, involving attack of the *N*-terminal amine on the central amide linkage to give bicyclic lactam **28**, is considerably more significant in the case of the pentamer **34** than the dimer **21** (Scheme 3). Thus the final step in the synthesis was achieved by treating Phth-T_5-Boc POM **34** with aqueous hydrochloric acid. Evaporation and lyophilisation gave Phth-T_5-POM **35**, as its HCl salt, which was greater than 95% pure as determined by analytical reverse phase HPLC (see ESI Fig. 4). All subsequent nucleic acid binding studies were carried out with this oligomer **35**, retaining the phthaloyl group. Subsequent as yet unpublished results have indicated that the *N*-terminal phthaloyl moiety has little effect on DNA/RNA binding properties compared with *N*-acetyl capped oligomers.

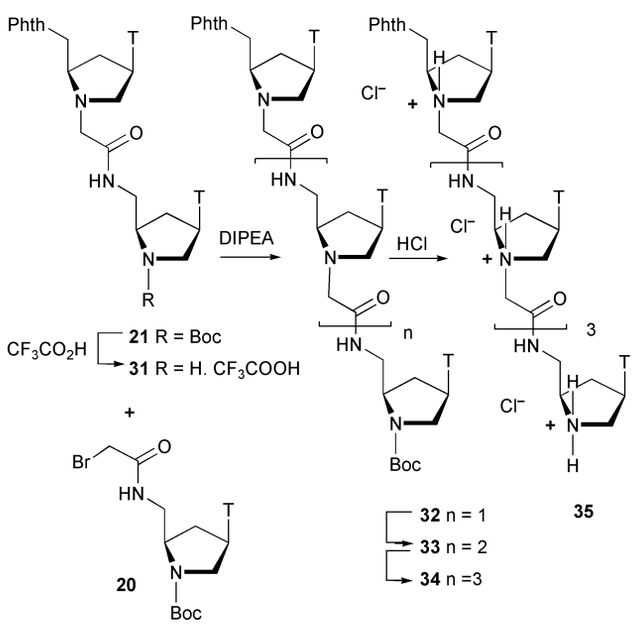

Scheme 4

UV spectroscopic analysis of T_5-POM–nucleic acid binding properties

Phth-T_5-POM binding poly(rA). UV thermal denaturation experiments were performed in order to evaluate the affinity of Phth-T_5-POM **35** upon hybridisation with RNA. Initially the variation of absorption (A_{260}) of an equimolar mixture of Phth-T_5-POM **35** and poly(rA) (42 μM each in bases) in 10 mM K_2HPO_4 buffer adjusted to 0.12 M K^+, pH 7.0, was recorded. A complete cycle of the thermal induced denaturation and renaturation involves fast heating (5 °C min^{-1}), slow cooling (0.2 °C min^{-1}), followed by slow heating (0.2 °C min^{-1}). The slow heating curve resulted in a single 26% hyperchromic shift with a melting temperature (T_m) of 48.5 °C (*ca.* 10 °C T_m/base) (Fig. 5a). Under identical conditions corresponding native $d(T)_5$ did not show any hyperchromic shift with poly(rA) above 8 °C, whilst the denaturation of $d(T)_{20}$ and poly(rA) has a T_m of 42.0 °C (*ca.* 2 °C T_m/base). A T_5-PNA containing a Lys residue at either terminus exhibits similar affinity for poly(rA), as Phth-T_5-POM **35**, with a T_m of 56 °C. While it is often hazardous to extrapolate a T_m value obtained with homo-oligomers into an accurate value of T_m per modification found in a mixed sequence, it is clear that Phth-T_5-POM **35** binds with extremely high affinity to poly(rA). Thus it would seem that the pyrrolidine ring imposes a favourable conformation for hybridisation with RNA. Based on results from modelling and NMR studies (*vide supra*) this is likely to be, at least in part, a result of the favourable northern C3′-*endo* type conformation adopted by the pyrrolidine ring.

Interestingly, substantial hysteresis was evident between the cooling and heating curves in this experiment (see ESI Fig. 6) indicating that the rate of heating/cooling employed (0.2 °C min^{-1}) is faster than the rate of association/dissociation of Phth-T_5-POM **35** and poly(rA) such that a true equilibrium is not attained. This is in contrast to native duplex forming nucleic acids which show essentially no hysteresis at this rate of temperature change, implying Phth-T_5-POM **35** hybridises more slowly to poly(rA) than do native nucleic acids. Since it is impossible to retrieve thermodynamic data unless the heating/cooling curves are coincident, an even slower rate of heating/cooling was employed. However, even at a heating/cooling rate of 0.1 °C min^{-1}, equilibrium conditions were still not realised. Thus in order to obtain a true equilibrium T_m value, an equimolar sample of Phth-T_5-POM **35** and poly(rA) was subjected to a series of cooling/heating ramps performed at five different rates (5, 2, 1, 0.5 and 0.1 °C min^{-1}). It was evident from these curves that the slower rates of annealing result in higher T_m values and greater hyperchromic shifts (see ESI Figs. 7 and 8). By extrapolating to an infinitely slow rate of heating/cooling, the true equilibrium T_m was determined to be 49 °C and is 0.5 °C higher than that observed at 0.2 °C min^{-1}. All further heating/cooling experiments were performed at 0.2 °C min^{-1} and so the quoted T_m values are slightly lower than the true equilibrium values and stand uncorrected.

Fidelity and stoichiometry of T_5-POM binding RNA. In order to assess the fidelity of Phth-T_5-POM **35** binding to RNA, UV denaturation experiments were carried out with **35** and the

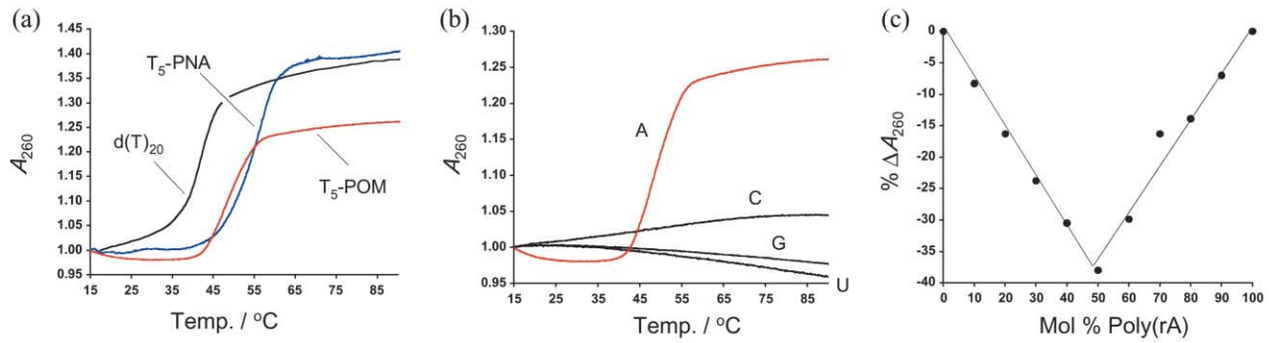

Fig. 5 (a) UV thermal denaturation curves of Phth-T_5-POM **35**, Lys-T_5-LysNH_2-PNA (*N*- and *C*-terminal Lys, with *C*-terminal amide) and $d(T)_{20}$ *vs*. poly(rA) (42 μM each in bases) in buffer A (10 mM K_2HPO_4) adjusted to 0.12 M K^+, pH 7.0. (b) UV thermal denaturation curves for Phth-T_5-POM **35** and an equimolar amount (42 μM each strand in bases) of poly(rA), (rU), (rC) or (rG) in buffer A adjusted to 0.12 M K^+, pH 7.0. (c) A Job plot of the % change in A_{260} *vs.* molar ratio Phth-T_5-POM **35** and poly(rA).

non-complementary homopolymers poly(rG), (rC) and (U) (Fig. 5b). In all three cases no significant hyperchromicity is observed, hence it can be concluded that Phth-T_5-POM **35** does not bind to the non-complementary homopolymers by a typical base-pairing/stacking mechanism. These results do not, however, rule out non-specific binding, *via* electrostatic interactions between the oppositely charged backbones.

A single hyperchromic shift was observed in the thermal denaturation of Phth-T_5-POM **35** and poly(rA) which is consistent with the melting of a Watson and Crick base paired duplex or the simultaneous dissociation of the three strands of a TA.T triple helix. In order to determine the binding stoichiometry and discriminate between these two possibilities the method of UV continuous variation was employed.[46] Here UV absorbance, over the range 220–300 nm, was measured as a function of the molar ratio of bases, for mixtures of Phth-T_5-POM **35** and poly(rA). An incubation period of 24 h prior to measurements was found to give the clearest results, presumably due to the relatively slow rate of association between **35** and poly(rA). A Job plot[46] of the percentage change in A_{260} against mole ratio of T : A shows a well-defined minimum at 1 : 1 consistent with duplex formation. In addition, the minimum in the Job plot occurs at the intersection of two straight lines, indicating a reversibly formed complex with few or no vacant sites.[47]

Effect of ionic strength and pH on T_m for Phth-T_5-POM binding RNA. Bruice and co-workers showed that decrease in ionic strength results in an increase in the binding affinity of the positively charged oligonucleotide DNG **5** (Fig. 1) to poly(dA) and poly(rA).[48,49] This is due the "intimate" association between the more "naked" oppositely charged backbones at lower salt concentration. In order to determine whether electrostatic attraction could contribute to the stability of the duplex formed between Phth-T_5-POM **35** and poly(rA), melting experiments were carried out at different ionic strength over a ten-fold concentration range. Surprisingly, there is actually a slight increase in duplex stability with increasing ionic strength between 0.12 and 1.2 M K^+ (T_m = 48.5 and 55.0 °C respectively), which equates to an increase in T_m/base of *ca*. 1 °C (Fig. 6a). This implies that electrostatic attraction is not a major contributing factor to the duplex stability. This may be a consequence of either there being a relatively large distance between the positive charge in POM and the negative charge of the phosphodiester group in a duplex with RNA, or that Phth-T_5-POM **35** is only partially protonated at pH 7.0. In addition, it may be that the observed increased affinity of **35** for poly(rA) at higher ionic strength is due to **35** adopting a slightly different conformation at higher salt concentration. It was also noticeable from the UV melting curves, recorded at different salt concentrations, that the hyperchromicity decreases significantly, whilst hysteresis between the heating and cooling curves

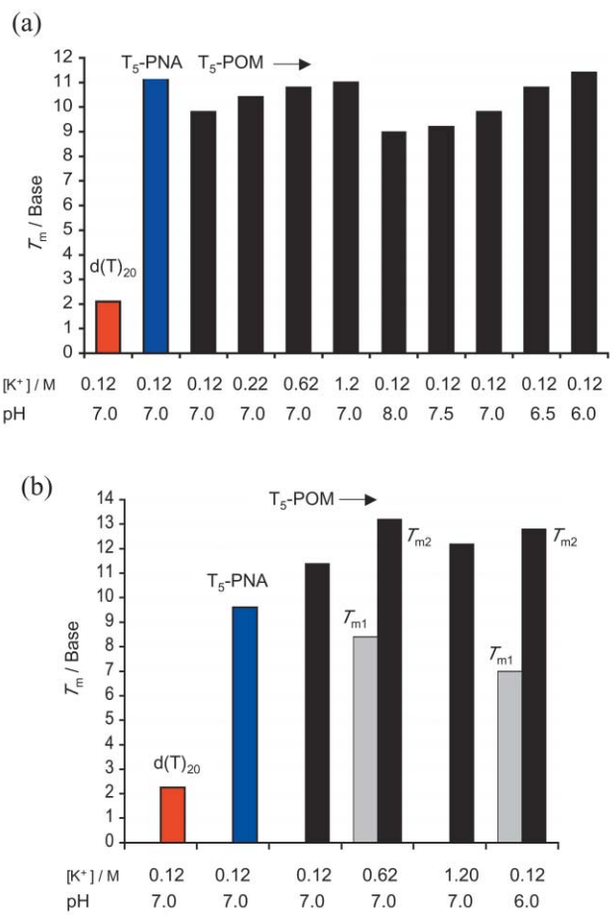

Fig. 6 (a) Transition melting temperatures per base (T_m/base) of Phth-T_5-POM **35**, Lys-T_5-LysNH_2-PNA and $d(T)_{20}$ with poly(rA) (42 μM each in bases) in buffer A (total volume 1 mL) adjusted to the appropriate ionic strength and pH. UV absorbance (A_{260}) was recorded with heating at 5 °C min^{-1} from 25 °C to 93 °C, cooling at 0.2 °C min^{-1} to 15 °C and heating at 0.2 °C min^{-1} to 93 °C. The T_m was determined from the first derivative of the final slow heating curve. (b) T_m/base for Phth-T_5-POM **35**, Lys-T_5-LysNH_2-PNA and $d(T)_{20}$ with poly(dA). As above except the mixture of **35** and poly(dA) (210 μM each in bases) was incubated for 48–96 h at 25 °C in buffer A (total volume 0.2 mL), diluted to 1 mL adjusting to the appropriate ionic strength and pH, cooled to 15 °C at 1 °C min^{-1}, heated at 0.2 °C min^{-1} to 93 °C from which the T_m was measured.

increases, at higher ionic strengths (see ESI Fig. 9). This is probably due to slower rates of association and dissociation at higher ionic strength.

In order to assess the effect of pH on the affinity of Phth-T_5-POM **35** binding to poly(rA), melting experiments were carried out at several different pH values over the range 6–8 (10 mM

phosphate buffer adjusted to 0.12 M K^+). This revealed that there is a substantial increase in T_m from 45 to 57 °C (ΔT_m/base = 2.1 °C) on lowering the pH from 8.0 to 6.0 (Fig. 6a). Thus, protonation of the nitrogen atom of the pyrrolidine ring is an important factor in the formation of more stable duplexes. The fact that duplex stability increases with salt concentration suggests that conformational changes brought about by protonation are more likely to be the cause of the observed increase in duplex stability at lower pH, than electrostatic attraction. From the melting curves (see ESI Fig. 10) it was again noticeable that greater hyperchromic shifts and reduced hysteresis are observed at lower pH, suggesting that binding occurs faster at lower pH. The fact that there was significant hysteresis between the heating and cooling curves even at pH 6.0 indicates binding is still slow relative to native duplex hybridisation.

Phth-T_5-POM binding DNA. In contrast to the distinct melting curves obtained with poly(rA), repeated UV heating/cooling experiments with an equimolar mixture (42 μM each in bases) of Phth-T_5-POM **35** and poly(dA) revealed no hyperchromic shifts between 15 and 93 °C. Surprisingly, a modest cooperative hyperchromic shift could be detected after a five-fold increased concentration of both **35** and poly(dA) (210 μM each in bases, total volume 200 μL) was incubated at 25 °C for 48 h, before the volume was readjusted to 1.0 mL (42 μM each in bases) (Fig. 7a). However, the T_m of 57.0 °C (11.4 °C/base) was only just detectable from the sloping baselines, indicating only a fraction of the single strands had fully annealed. Thus Phth-T_5-POM **35** can hybridise with poly(rA) in the order of minutes (at 42 μM each in bases), but remarkably only partially hybridises with poly(dA) at a five-fold increased concentration after an extended period of 2 days incubation. It is also of note that although Phth-T_5-POM **35** binds extremely slowly to poly(dA), it does so with a higher affinity than for poly(rA) (increase in T_m of 8 °C at 0.12 M K^+, pH 7.0). In addition, **35** binds to poly(dA) with higher affinity compared to Lys-T_5-Lys-PNA, which gave rise to a T_m of 48 °C (9.6 °C/base). All subsequent T_m values for equimolar mixtures of **35** and poly(dA) were obtained by incubating the two complementary strands at a five-fold increased concentration (210 μM each in bases) for at least 48 h prior to diluting the sample five-fold. While obtaining T_m values with poly(dA) proved more difficult than with poly(rA), the trends appear the same for both series (Fig. 6b). Phth-T_5-POM **35** binds to poly(dA) with higher affinity at higher ionic strength and lower pH. In some cases two hyperchromic shifts could be detected, suggesting triplex formation. However, due to the extremely slow binding kinetics, the stoichiometry of binding could not be satisfactorily determined, using the method of UV continuous variation. Indeed, although the Job plot for **35** and poly(dA), obtained at an ionic strength of 0.12 M and pH 7.0, gave a minimum at approximately 30% T indicative of a TA.T triplex, this was poorly defined.

Following our initial communication of POM,[25] it was reported that incorporation of either one or two thymidylpyrrolidine units, with the same stereochemistry as POM (2′*R*,4′*R*), into ssDNA results in substantially destabilised duplexes and triplexes, relative to wild-type, upon hybridisation with complementary ssDNA and dsDNA, respectively.[39] Our results using a fully modified Phth-T_5-POM **35** thus highlight that it is clearly very hazardous, and unadvisable, to extrapolate T_m values based on such a simple chimeric approach as a means for understanding the nucleic acid binding properties of fully modified novel nucleic acid mimics.

UV kinetic analysis of Phth-T_5-POM binding DNA and RNA

Phth-T_5-POM binds faster to RNA than DNA. Since UV thermal denaturation experiments suggested there to be a substantial kinetic selectivity for Phth-T_5-POM **35** binding to poly(rA) over poly(dA), we decided to monitor the binding events as a function of time. Initially absorbance changes at 260 nm were monitored at 25 °C immediately upon mixing an equimolar amount of **35** into a buffered solution containing either poly(rA) or poly(dA) (42 μM each in bases, 0.12 M K^+, pH 7.0). Under these conditions an hypochromic shift of 29% was observed after 200 min upon mixing **35** with poly(rA) (Fig. 7b). However when **35** was similarly mixed with poly(dA) no drop in A_{260} was observed even after 16 h. It was only after increasing the concentration of each strand five-fold to 210 μM (in bases), that hybridisation between Phth-T_5-POM and poly(dA) can be observed. At this elevated concentration a moderate absorbance drop of only *ca.* 6% was observed after 200 min, remarkably A_{260} was still dropping even after 12 h. These experiments clearly confirm that Phth-T_5-POM **35** binds much faster to RNA than DNA. Overall, however, it is also evident that binding of Phth-T_5-POM to poly(rA) is slow when compared with Lys-T_5-Lys-PNA. In an identical UV kinetic experiment PNA hybridisation with poly(rA) (42 μM each in bases) is essentially complete after 10 minutes, whilst Phth-T_5-

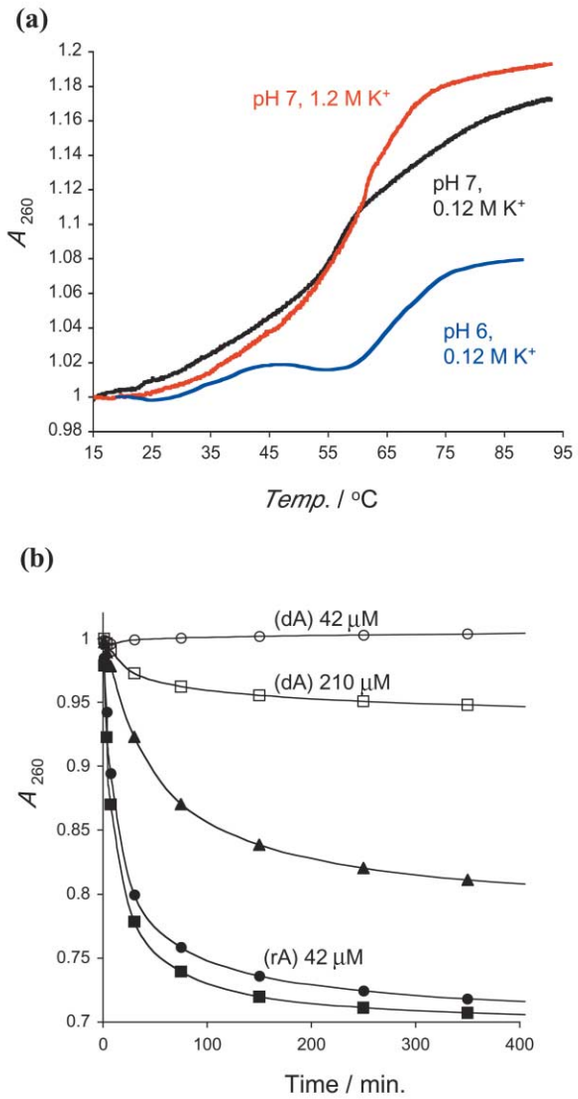

Fig. 7 (a) UV thermal denaturation curves of Phth-T_5-POM **35** *vs.* poly(dA) following incubation for 48–96 h at 25 °C in buffer A (210 μM each in bases, 0.2 mL), five-fold dilution and adjustment of ionic strength and pH. (b) Normalised UV absorbance (A_{260}) of Phth-T_5-POM **35** with poly(rA) and (dA) *vs.* time at 25 °C. **35** and poly(dA) (42 μM each in bases), 0.12 M K^+, pH 7 (○); **35** and poly(dA) (210 μM), 0.12 M K^+, pH 7 (□); **35** and poly(rA) (42 μM), 0.22 M K^+, pH 7 (▲); **35** and poly(rA) (42 μM), 0.12 M K^+, pH 7 (●); **35** and poly(rA) (42 μM), 0.12 M K^+, pH 6 (■).

POM fails to reach equilibrium even after 100 minutes (see ESI Fig. 11).

To the best of our knowledge, there have been no reports of a kinetically selective sequence specific association of a ligand for RNA over ssDNA (or *vice-versa*). However other systems have been reported to display weak but thermodynamically selective binding for single stranded RNA over DNA. For example, 2′,5′-linked RNA,[50] 2′,5′-linked DNA[51] and 2′,5′-linked thioformacetal-modified[52] oligonucleotides all show substantial thermodynamic selectivity for hetero-duplex formation with RNA over ssDNA, albeit they bind with lower affinity to complementary RNA than do the corresponding isosequential DNA oligonucleotides. At present we have no satisfactory model to explain this kinetic selectivity of Phth-T_5-POM for poly(rA) over poly(dA) and further studies will be required to delineate the mechanism of binding. Perhaps binding of Phth-T_5-POM to poly(dA) induces a major conformational change to poly(dA) (or *vice-versa*), which retards further binding. It is noteworthy that a chiral PNA thymidyl decamer with a (2*R*,4*R*)-*N*-aminoethyl-D-proline backbone reported by Vilaivan *et al.*,[37] which differs only in the position of the amide group in the backbone, was also found to bind selectively to poly(rA) and not poly(dA). However, no investigation into binding kinetics was reported and it is thus tempting to postulate that longer incubation times would likewise reveal some binding to poly(dA). Ganesh and co-workers found no such selectivity with the stereoisomers (2*S*,4*S*) and (2*R*,4*S*) of this *N*-aminoethyl proline based oligomer.[38] However, these oligomers[38] were chimeras with just one pyrrolidine unit incorporated in a standard PNA strand. Thus any conclusions that were drawn from this work[38] are, at best, fragile.

Ionic strength and pH also affect the rates of hybridisation. Similar UV kinetic experiments were also carried out to determine the effects of changing ionic strength and pH on the kinetics of Phth-T_5-POM **35** binding poly(rA) (see Fig. 7b and ESI Figs. 12 and 13). This reveals that binding is much faster at lower ionic strengths. This confirms that greater hyperchromic shifts observed in the UV thermal denaturation of Phth-T_5-POM **35**/poly(rA) duplexes (*vide supra*) at lower ionic strengths must arise from a higher percentage of duplex formed on annealing due to faster rates of association. Furthermore, these results suggest that electrostatic interactions are important in determining the kinetics of duplex formation. The results for Phth-T_5-POM **35** binding poly(rA) at different pHs also confirm that binding is faster at pH 6 than at pH 7, which in turn, is considerably faster than at pH 8. It is also noticeable that the rates of binding are much less sensitive to pH than to ionic strength. Unfortunately, the hybridisation of **35** with poly(rA) did not obey either first order or *pseudo* first-order kinetics. Indeed no quantitative kinetic analysis was performed using this data since as far as we are aware, no model exists to account for the binding of a short ligand containing several identical binding domains to a target bearing many potential binding sites of which the degree of occupancy is unknown.[53]

SPR analysis

Since UV spectroscopy can only detect changes in base stacking interactions, it cannot be used to unequivocally ascertain the specificity of binding of modified oligonucleotides to nucleic acids. This was a particular concern since any non-specific electrostatic backbone interactions between Phth-T_5-POM **35** and complementary or non-complementary nucleic acids need not involve a change in the extent of base-stacking. Surface Plasmon Resonance (SPR) is a technique which is gaining popularity for studying biomolecular interactions.[54–56] Whilst it has rarely been used for the study of modified oligonucleotide–nucleic acid interactions, it can give rapid insight into kinetics and thermodynamics and thus binding specificity.[56] It was also chosen as a complementary technique to UV spectroscopy in order to observe more readily the slow interaction between Phth-T_5-POM **35** and poly(dA) since SPR permits the use of higher analyte concentrations than is possible with UV spectroscopy. Accordingly 5′-biotinylated targets, $d(A)_{20}$ and $r(A)_{20}$, were immobilised onto a streptavidin loaded carboxymethyl-dextran matrix of a standard SPR sensor chip (Biacore, Stevenage). To ensure an equivalent number of binding sites, $d(A)_{20}$ and $r(A)_{20}$ were injected across flow cells 2 and 3 of the four compartment sensor chip to give values of 1400 and 1450 response units (RU), respectively. In order to ensure against non-specific electrostatic interactions that may have arisen from the interaction between positively charged Phth-T_5-POM **35** and the negatively charged carboxylate surface of the matrix, one surface (flow cell 1) was left underivatised. In addition, as a control of Phth-T_5-POM **35** binding specificity, the surface of flow cell 4 was derivatised with an ssDNA of mixed sequence, 5′-biotin-d(AGC TTC AGA GAT CGA TCG GAG AGA GTA CTG) (*NFκB*), to a value of 1000 RU. Having immobilised the native oligonucleotides, Phth-T_5-POM **35** was injected at different concentrations across all four flow cells of the sensor surface using a 10 mM K_2HPO_4 buffer adjusted to 0.12 M K^+ and pH 7.0. Typically, Phth-T_5-POM **35** was injected across the surfaces for 300 s followed by buffer alone. After this dissociation phase, the surface was regenerated and any excess **35** was removed, by injecting a pulse of 10 mM HCl across the surfaces.

Fig. 8a shows the sensogram obtained at a concentration of 40 μM and shows clearly that while Phth-T_5-POM **35** associates with $d(A)_{20}$, it does so considerably slower than to $r(A)_{20}$. Phth-T_5-POM **35** also shows no significant binding to the negatively charged carboxymethyl dextran matrix, confirming the feasibility of using this type of sensor surface. Crucially, no binding was observed to the mixed sequence control (*NFκB*), above background, demonstrating that Phth-T_5-POM **35** retains the high fidelity of base pair recognition displayed by native nucleic acids and does not exhibit any non-specific binding through electrostatic interactions. Furthermore when the concentration of Phth-T_5-POM **35** injected was increased two-fold (80 μM, Fig. 8b) there was still no binding to the mixed sequence control, above the background. These results are also significant in that they prove that the hypochromic shifts observed upon hybridising Phth-T_5-POM **35** with poly(dA) compared to poly(rA) are not an artefact of poor base stacking within the Phth-T_5-POM/poly(dA) complex relative to that of the Phth-T_5-POM/poly(rA) complex, but are due to a difference in relative rates of association.

As a comparison, $d(T)_5$ was injected across the sensor surfaces. As expected, no duplex formation was observed with $d(A)_{20}$ or $r(A)_{20}$ at concentrations even as high as 160 μM. This clearly reflects the much higher binding affinity of Phth-T_5-POM **35** compared with its DNA 5mer counterpart.

The effect of ionic strength on the rates of association and dissociation of Phth-T_5-POM with $d(A)_{20}$ and $r(A)_{20}$ was investigated using a buffer with an increase in KCl concentration. This reveals that the rates of association to both $r(A)_{20}$ and $d(A)_{20}$ are very much reduced at higher ionic strength (see ESI Fig. 14), consistent with observations obtained by UV spectroscopy. As postulated previously, this is most likely due to diminished inter-strand electrostatic attraction since the oppositely charged backbones will effectively be shielded from one another by the presence of more counter ions in the solution. However, it is also possible that conformational differences arise at higher ionic strength which could be responsible for this difference. Again, faster binding is observed to $r(A)_{20}$ than to $d(A)_{20}$ at higher ionic strength, albeit the difference is slightly diminished compared with a buffer of low ionic strength. Nonetheless, this shows that the factors responsible for the

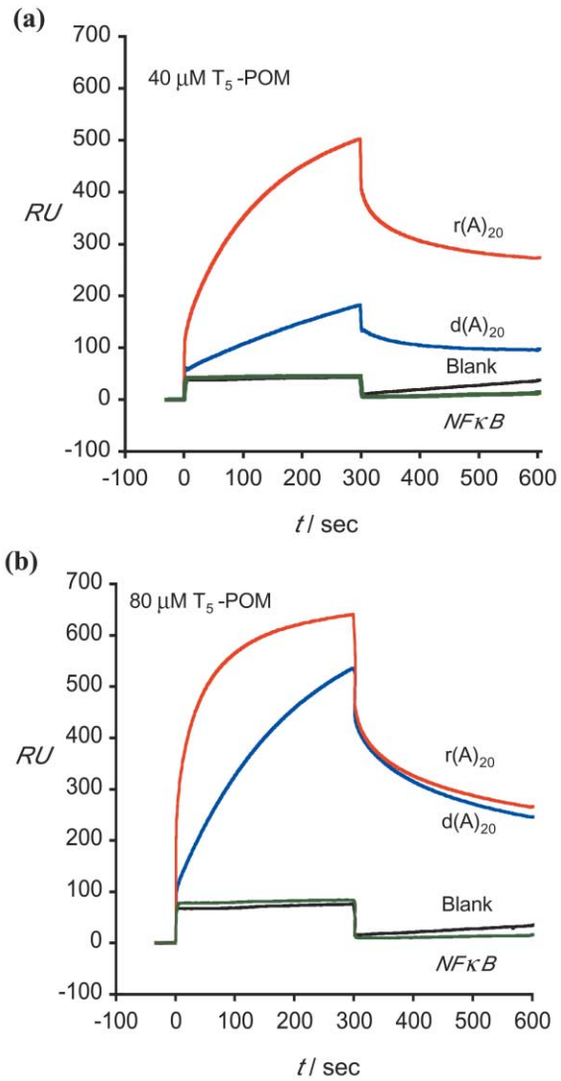

Fig. 8 SPR response (*RU*) *vs*. time for Phth-T_5-POM **35** injected across $r(A)_{20}$, $d(A)_{20}$, d(AGC TTC AGA GAT CGA TCG GAG AGA GTA GTG-3′) derivatised surfaces and an underivatised control surface. Response profiles were determined using a BIAcore 2000 instrument (Biacore AB, UK) under standard conditions following injection of Phth-T_5-POM **35** (a) 40 μM and (b) 80 μM strand concentration (in buffer A, pH 7 adjusted to 0.12 M K^+) across each surface at a flow rate of 20 μL min^{-1} for 300 s, followed by buffer to allow dissociation. All oligonucleotides were biotinylated at the 5′-end (Cruachem, UK) and immobilised on a streptavidin derivatised carboxymethyl dextran sensor chip (Biacore).

kinetic selectivity of Phth-T_5-POM **35** for binding RNA over ssDNA are largely independent of ionic strength.

Next the effect of pH on the rates of association, dissociation and specificity of binding of Phth-T_5-POM **35** with immobilised native oligonucleotides was investigated. This revealed that the overall trends at pH 6.0 are very similar to those at pH 7.0, with Phth-T_5-POM **35** binding much faster to $r(A)_{20}$ relative to $d(A)_{20}$ (see ESI Fig. 15). Thus the factors responsible for the kinetic selectivity prevail even at lower pH. Faster binding to both targets was also observed at pH 6.0 compared with that at pH 7.0, and is in agreement with the UV spectroscopic measurements. This is likely to be a consequence of enhanced electrostatic attraction between the more protonated Phth-T_5-POM and target nucleic acids. Notably, lowering the pH to 6.0 does not result in any non-specific binding to the mixed sequence above the background response of the underivatised surface. However, when the same experiments were performed at pH 5.0 (0.12 M K^+), substantial binding to the mixed sequence ssDNA (*NFκB*) was observed whereas very little binding to the dextran was detected (see ESI Fig. 16). A fast rate of dissociation from *NFκB* is also observed, implying that the binding is weak. Thus at pH 5.0, weak, non-specific interactions occur between Phth-T_5-POM **35** and ssDNA, presumably arising from electrostatic attraction, such that the specific Watson–Crick type base-pairing is disrupted. This also represents the first example of a modified oligonucleotide capable of switching from sequence specific to sequence non-specific binding of a nucleic acid under the control of an external stimulus (pH). Finally it is noteworthy that the rate of dissociation of Phth-T_5-POM **35** from the mixed sequence ssDNA (*NFκB)* at pH 5.0 is much faster than from $d(A)_{20}$, suggesting that, in the presence of a complementary sequence, Phth-T_5-POM binds to $d(A)_{20}$ preferentially *via* Watson–Crick type base-pairing.

Summary

An efficient synthetic route to the highly water-soluble cationic dinucleotide analogue T_2-POM **30**, has been developed. ^{1}H NMR spectroscopy has shown that the *N*-acetamido group of the protonated pyrrolidine ring in POM adopts a preferred *trans*-configuration relative to the base and thus the backbone is stereochemically equivalent to native nucleic acids. Semi-empirical quantum mechanical calculations carried out on dimethylpyrrolidine nucleoside analogues also support this observation. In addition, it was found that the pyrrolidine ring preferentially adopts a conformation similar to the northern-type conformation adopted by ribose in RNA. Moreover, since the thymine base was found to be suitably oriented for intermolecular hydrogen bonding, thymidyl POM satisfies the necessary configurational and conformational requirements for hybridisation with DNA and RNA.

Oligonucleotide analogues comprised of a pyrrolidine-amide backbone are emerging as a new class of nucleic acid mimics with desirable properties.[36,37,40] Our preliminary studies have found that the pyrrolidine-amide oligonucleotide mimics (POM), in particular, exhibit many desirable, as well as unforeseen properties. Solution-phase synthesis of the highly water soluble thymidyl pentamer Phth-T_5-POM was achieved using an efficient iterative *N*-alkylation strategy. UV spectroscopy and surface plasmon resonance have shown that Phth-T_5-POM binds with very high affinity and specificity to complementary ssDNA and RNA. Surprisingly, upon increasing the ionic strength, slightly elevated T_m's were observed, suggesting that electrostatic attraction between oppositely charged backbones does not play a significant role in binding affinity. Decreasing the pH resulted in elevated T_m's which is possibly a consequence of conformational changes brought about by protonation of the pyrrolidine ring. By contrast, Phth-T_5-POM was found to bind to complementary RNA faster at lower ionic strength and pH, implying that electrostatic interactions are important in determining the kinetics of hybridisation. SPR analysis has also shown unequivocally that Phth-T_5-POM maintains the fidelity of sequence specific binding (base-pairing) observed with native nucleic acids, at both pH 7.0 and 6.0. However, at pH 5.0 the cationic oligonucleotide was attracted to a non-complementary ssDNA, presumably *via* electrostatic contacts between oppositely charged backbones. Intriguingly, Phth-T_5-POM was found to bind much faster to RNA than to DNA. We are currently developing a solid-phase synthesis of longer mixed sequence POM in order to explore in greater depth this kinetically selective recognition, which may provide new insight into the conformational differences between the two native nucleic acid forms.

Experimental section

^{1}H NMR spectra were recorded at 270, 300, 400 or 500 MHz. ^{13}C NMR spectra were recorded at 67.9, 75.5, or 100.6 MHz. Chemical shifts are reported in parts per million relative to Me_4Si or residual solvent signal. ^{19}F NMR spectra were

recorded at 188.2 MHz unreferenced. FAB mass spectra were obtained on a ZAB-SE VG Analytical Fisons Instrument. Electron Impact (EI) and Chemical Ionisation (CI) mass spectra were recorded using a VG Analytical 70 70 EQ mass spectrometer using NH_3 as carrier gas. Electrospray ionisation (ESI) mass spectra were performed, in positive ion mode, using a Q-Tof (Micromass, Manchester). Infra-red spectra were acquired on a Perkin-Elmer 783 as KBr discs or $CHCl_3$ solutions. Melting points were determined using a Cambridge Instrumental microscope with a Reichert-Jung heating mantle and are uncorrected. Optical rotations were measured at 20 °C with an Optical Activity AA-1000 polarimeter. Flash silica column chromatography was carried out over Merck Kieselgel 60 (230–400 mesh) and Merck Kieselgel 60 F254 0.25 mm plates were used for analytical TLC. Reactions involving anhydrous conditions were carried out in flame-dried glassware under a positive pressure of argon. All solvents were distilled before use. Reagents were purified and solvents dried using standard procedures.

Molecular modelling

Co-ordinates of X-ray crystal structures of uridine **7**[32] and a pyrrolidine HCl salt **6**[29] (Fig. 2) were obtained from the Cambridge Crystallographic Database. The pseudorotation phase angle (*P*) and degree of pucker or maximum torsional angle (ν_{max}) are calculated by substituting the published torsion angles ($\nu_0 \longrightarrow \nu_4$) into the equations: Tan $P = \{(\nu_4 + \nu_1) - (\nu_3 + \nu_0)\}/\{2 \cdot \nu_2 \cdot (\sin 36° + \sin 72°)\}$and $\nu_{max} = \nu_2/\cos P$.[30,31] Models of the *cis*- and *trans*-dimethylpyrrolidines **8** and **9** (Fig. 3) were built from the co-ordinates of the reported crystal structure of pyrrolidine **6**. For both diastereoisomers 35 conformations, for every 10 degrees of pseudorotation, were energy minimised, allowing only free rotation of the thymine base about the C4′–N1 bond, in order to optimise the C3′–C4′–N1–O2 torsion angle which is analogous to the glycosyl torsion angle in native nucleic acids (χ).[31] The enthalpies of formation for each conformer were then calculated by semi-empirical quantum mechanical calculations using MOPAC 6.0 software[41] on a Silicon Graphics workstation. The maximum torsional angle (ν_{max}) was optimised to 40°. The standard enthalpies of formation, phase angles (*P*), cyclic torsion angles $\nu_0 \longrightarrow \nu_4$, and the torsion angle C3′–C4′–N1–C2 (χ for conformers **A**–**D**) are shown in ESI (Table 1). The structures of conformers **A** and **B** are shown in Fig. 4.

NMR conformational analysis

NMR spectra of T_2-POM·3HCl **30** (*ca.* 4 mg) dissolved in 99.9% D_2O (0.5 ml) were recorded at 500 MHz on a Bruker DRX500 at 30 °C and referenced to the residual HDO peak at 4.70 ppm. A ^{1}H spectral width of 5000 Hz was used throughout. 2D TOCSY, COSY 45, ROESY and *J*-resolved spectra were collected using 8k data points in t_2 and 256 t_1 increments, typically zero-filled to 8k × 512 data points, with a relaxation delay of 2 seconds. Suppression of residual solvent signal (HDO) was achieved using presaturation during the relaxation delay. ROESY and TOCSY spectra had typical mixing times of 300 and 60 ms respectively. The assignment of all proton chemical shifts, vicinal coupling constants, and ROESY cross peaks are given in ESI. The observed $^3J_{HH}$ coupling constants for the tri-substituted (upper) pyrrolidine ring of T_2-POM·3HCl **30** (Table 1) were compared with the calculated $^3J_{HH}$ coupling constants for the corresponding vicinal protons for the lowest energy conformers **A**–**D** of the model *cis*- and *trans*-dimethylpyrrolidines **8** and **9** (Fig. 3). The calculated $^3J_{HH}$ coupling constants are derived from the general Karplus equation $J_j = a_j \cos^2 \phi + b_j \cos \phi + c_j$.[45] The Karplus parameters used in the calculations, a_j, b_j and c_j, are listed in Table 1 and are the same as those derived for L-4-hydroxyproline.[45]

***N*-(*tert*-Butoxycarbonyl)-*trans*-4-formyloxy-D-proline ethyl ester.** Ph_3P (9.47 g, 36.0 mmol), followed by dry formic acid (1.4 mL, 37.0 mmol), was added to a stirred solution of *N*-(*tert*-butoxycarbonyl)-*cis*-4-hydroxy-D-proline ethyl ester **10**[42] (7.6 g, 29.0 mmol) in dry THF (125 mL) under argon. The mixture was then cooled to −20 °C and diisopropyl azodicarboxylate (DIAD) (7.3 mL, 37.0 mmol) was added dropwise over 30 min. The solution was held at −20 °C for a further 15 min and then allowed to warm to room temperature and stirred for a further 18 h. The resulting yellow solution was evaporated under reduced pressure, and Et_2O (*ca.* 50 mL) was added to precipitate triphenylphosphine oxide which was removed by filtration. The filtrate was evaporated under reduced pressure and the residue was purified by flash chromatography, eluting with 5% acetone in CH_2Cl_2, to give the title compound (7.62 g, 90%) as a pale yellow oil. R_f 0.28 (5% acetone in CH_2Cl_2); $[\alpha]_D$ +46.5 (*c* = 2.0, EtOH); δ_H (300 MHz, $CDCl_3$) 1.28–1.38 (3H, m, CH_2CH_3), 1.44 and 1.47 (total 9H, 2 × s, $C(CH_3)_3$ rotamers), 2.20–2.29 (1H, m, H_a3), 2.39–2.49 (1H, m, H_b3), 3.58–3.74 (2H, m, H5), 4.22 (2H, q, *J* 7.0, CH_2CH_3), 4.34–4.47 (1H, 2 × t, each *J* 7.9, H2 rotamers), 5.43 (1H, br s, H4), 8.02 and 9.21 (total 1H, 2 × s, HCO rotamers); δ_C (100.6 MHz, $CDCl_3$) 14.5 (CH_2CH_3), 28.6 and 28.7 ($C(CH_3)_3$ rotamers), 35.8 and 36.9 (C3 rotamers), 52.2 and 52.5 (C5 rotamers), 57.9 and 58.2 (C2 rotamers), 61.6 (CH_2CH_3), 71.1 and 72.0 (C4 rotamers), 81.0 ($C(CH_3)_3$), 153.9 and 154.4 ($CO_2{}^t$Bu rotamers), 160.4 and 160.5 (HCO_2 rotamers), 172.6 and 172.8 (CO_2Et rotamers); *m*/*z* (FAB$^+$) 288 ([M + H]$^+$, 53%), 260 (45), 232 (47), 188 (63); HRMS *m*/*z* (CI) 288.1451 ([M + H]$^+$, $C_{13}H_{22}NO_6$ requires *m*/*z,* 288.1447).

***N*-(*tert*-Butoxycarbonyl)-*trans*-4-hydroxy-D-proline ethyl ester.** 25% aq. NH_3 (1.8 mL) was added to a solution of *N*-(*tert*-butoxycarbonyl)-*trans*-4-formyloxy-D-proline ethyl ester (3.50 g, 13.4 mmol) in CH_3OH (30 mL) and the mixture was then stirred at room temperature for 5 h. Evaporation of solvent under reduced pressure and subsequent purification by flash chromatography, using ethyl acetate as eluant, gave the title compound (2.90 g, 91%) as a viscous transparent oil. R_f 0.35 (3 : 1 ethyl acetate–hexane); $[\alpha]_D$ +67.4 (*c* = 2.0, EtOH) [lit.[42] $[\alpha]_D$ +70.4 (*c* = 2.0, EtOH)]; δ_H (300 MHz, $CDCl_3$) 1.28 (3H, t, *J* 7.2, CH_2CH_3), 1.41 and 1.46 (total 9H, 2 × s, $C(CH_3)_3$ rotamers), 2.00–2.17 (1H, m, H_a3), 2.18–2.65 (2H, m, H_b3 and OH), 3.40–3.71 (2H, m, H5), 4.17 and 4.18 (total 2H, 2 × q, *J* 7.2, CH_2CH_3 rotamers), 4.32–4.44 (1H, m, H2), 4.45–4.53 (1H, m, H4); δ_C (100.6 MHz, $CDCl_3$) 14.6 (CH_2CH_3), 28.6 ($C(CH_3)_3$), 38.8 and 39.5 (C3 rotamers), 55.1 (C5), 58.1 and 58.4 (C2 rotamers), 61.4 (CH_2CH_3), 69.7 and 70.5 (C4 rotamers), 80.7 ($C(CH_3)_3$), 154.5 ($CO_2{}^t$Bu), 173.3 and 173.5 (CO_2Et rotamers); *m*/*z* (FAB$^+$) 260 ([M + H]$^+$, 50%), 204 (96), 160 (100); HRMS *m*/*z* (CI) 260.1501 ([M + H]$^+$, $C_{12}H_{22}NO_5$ requires *m*/*z,* 260.1498).

***cis*-4′-(*N*^{3}-Benzoylthymin-1-yl)-*N*-(*tert*-butoxycarbonyl)-D-proline ethyl ester (11).** Diethyl azodicarboxylate (DEAD) (1.0 mL, 6.37 mmol) was added dropwise over 1 h to a solution of *N*-(*tert*-butoxycarbonyl)-*trans*-4-hydroxy-D-proline ethyl ester (1.50 g, 5.79 mmol), *N*^{3}-benzoylthymine[33] (1.33 g, 5.79 mmol) and Ph_3P (1.72 g, 6.37 mmol) in THF (50 mL) at −15 °C. The mixture was warmed to room temperature and stirred for 18 h. Evaporation under reduced pressure and purification by column chromatography, eluting with 5% acetone in CH_2Cl_2 and then 5% CH_3OH in CH_2Cl_2, gave the ester **11** (1.69 g, 62%) as a white foam. R_f 0.70 (5 : 1 CH_2Cl_2–acetone); $[\alpha]_D$ +9.9 (*c* = 2.0, CH_2Cl_2); ν_{max} (KBr)/cm^{-1} 1731 and 1692 (CO); λ_{max} (CH_3OH)/nm 270 (ε/dm^3 mol^{-1} cm^{-1} 11000); δ_H (300 MHz, $CDCl_3$) 1.24 (3H, t, *J* 7.1, CH_2CH_3), 1.35 and 1.39 (total 9H, 2 × s, $C(CH_3)_3$), 1.92 (3H, d, *J* 0.8, thymine CH_3), 1.97–2.14 (1H, m, H_a3'), 2.65–2.83 (1H, m, H_b3'), 3.38–3.71 (1H, m, H_a5'), 3.90 (1H, dd, *J* 11.9, 7.7, H_b5'), 4.17 (2H, q, *J* 7.1,

CH_2CH_3), 4.22–4.43 (1H, m, H2′), 5.18 and 5.35 (total 1H, 2 × br s, H4′ rotamers), 7.31 (1H, s, H6), 7.42 (2H, t, *J* 7.5, Bz *m*-H), 7.58 (1H, t, *J* 7.5, Bz *p*-H), 7.84 (2H, d, *J* 7.1, Bz *o*-H); δ_C (100.6 MHz, $CDCl_3$) 12.5 and 13.0 (thymine CH_3 rotamers), 14.6 (CH_2CH_3), 28.6 ($C(CH_3)_3$), 36.1 and 36.5 (C3′ rotamers), 49.9 (C5′), 52.8 (C4′), 57.9 (C2′), 61.6 and 62.0 (CH_2CH_3 rotamers), 81.6 ($C(CH_3)_3$), 112.1 (C5), 129.1 and 129.5 (Bz *m*-C rotamers), 130.8 (Bz *o*-C), 132.0 (Bz *ipso*-C), 135.4 (C6), 136.4 (Bz *p*-C), 150.3 (C2), 153.8 and 154.1 ($CO_2{}^t$Bu rotamers), 162.2 and 162.8 (C4 rotamers), 169.2 (COPh), 172.8 (CO_2Et); *m*/*z* (FAB^+) 472 ($[M + H]^+$, 20%), 416 (36), 372 (20); HRMS *m*/*z* (CI) 472.2081 ($[M + H]^+$, $C_{24}H_{30}N_3O_7$ requires *m*/*z,* 472.2083).

***N*-(*tert*-Butoxycarbonyl)-*cis*-4′-(thymin-1-yl)-D-prolinol (12).** Lithium borohydride (49 mg, 2.24 mmol) was added portionwise over 1 h to a solution of ethyl ester **11** (0.53 g, 1.12 mmol) in dry THF (10 mL) at 0 °C. Stirring was continued at 0 °C for a further 30 min, then the mixture was allowed to warm to room temperature and stirred overnight. The reaction was cooled to 0 °C, quenched by the addition of methanol (20 mL), and evaporated under reduced pressure. Saturated aq. NaCl (20 mL) was then added and the mixture was extracted with $CHCl_3$–EtOH (2 : 1 v/v, 6 × 20 mL), dried over anhydrous $MgSO_4$, filtered and evaporated under reduced pressure. Purification by column chromatography, eluting with 5% CH_3OH in CH_2Cl_2, gave the alcohol **12** (0.250 g, 69%) as a white solid. R_f 0.12 (5% CH_3OH in CH_2Cl_2); mp 79–81 °C (from hexane–ethyl acetate); $[\alpha]_D$ +10.6 (*c* = 2.0, CH_2Cl_2); ν_{max} (KBr)/cm^{-1} 3412 and 3188 (OH), 1689 (CO); λ_{max} (CH_3OH)/nm 270 (ε/dm^3 mol^{-1} cm^{-1} 8800); δ_H (300 MHz, $CDCl_3$) 1.49 (9H, s, $C(CH_3)_3$), 1.96–2.00 (4H, m, thymine CH_3 and H_a3'), 2.40–2.49 (1H, m, H_b3'), 3.27 (1H, dd, *J* 10.9, 9.8, H_a5'), 3.69 (1H, dd, *J* 11.3, 5.6, CH_aH_bOH), 3.92 (1H, d, *J* 10.9, H_a5'), 3.98–4.10 (2H, m, CH_aH_bOH and H2′), 5.05–5.11 (1H, m, H4′), 7.13 (1H, s, H6), 8.25 (1H, s, H3); δ_C (67.9 MHz, $CDCl_3$) 12.5 (thymine CH_3), 28.3 ($C(CH_3)_3$), 32.2 (C3′), 49.8 (C5′), 51.8 (C4′), 58.6 (C2′), 65.5 (CH_2OH), 81.2 ($C(CH_3)_3$), 111.7 (C5), 135.9 (C6), 151.1 (C2), 155.9 ($CO_2{}^t$Bu), 163.4 (C4); *m*/*z* (FAB^+) 348 ($[M + Na]^+$, 25%), 326 ($[M + H]^+$, 43), 270 (64), 226 (100); HRMS *m*/*z* (FAB^+) 326.1717 ($[M + H]^+$, $C_{15}H_{24}N_3O_5$ requires *m*/*z,* 326.1716).

***N*-*tert*-Butoxycarbonyl-*cis*-4′-(thymin-1-yl)-D-prolinol *p*-toluenesulfonate (15).** Tosyl chloride (121 mg, 0.63 mmol) was added to a solution of alcohol **12** (103 mg, 0.32 mmol) in dry pyridine (1.0 mL) at 0 °C and the mixture was stirred for 15 min, allowed to warm to room temperature and stirred for a further 18 h. CH_3OH (10 mL) and water (5 mL) were slowly added and the mixture was then evaporated under reduced pressure. Purification by flash chromatography (0⟶10% CH_3OH in CH_2Cl_2) gave the tosyl derivative **15** (150 mg, 99%) as a white foam. $[\alpha]_D$ +5.8 (*c* = 0.12, CH_2Cl_2); ν_{max} (KBr)/cm^{-1} 1700 br (C=O), 1400 (SO_2 and $C(CH_3)_3$), 1385 ($C(CH_3)_3$), 1165 (SO_2), 807 (Ar-H); δ_H (270 MHz, $CDCl_3$) 1.32 (9H, s, $C(CH_3)_3$), 1.91 (3H, s, thymine-CH_3), 1.93–2.14 (1H, m, H_a3'), 2.38 (3H, s, Ar-CH_3), 2.45–2.58 (1H, m, H_b3'), 3.05–3.20 (1H, m, H_a5'), 3.86–3.94 (1H, m, H_b5'), 4.00–4.15 (2H, m, CH_2OSO_2), 4.22–4.55 (1H, m, H2′), 5.00–5.23 (1H, m, H4′), 7.19 (1H, br s, H6), 7.36 (2H, d, *J* 8.3, Ar), 7.78 (2H, d, *J* 8.3, Ar), 9.34 (1H, s, NH); δ_C (67.9 MHz, $CDCl_3$) 12.5 (thymine CH_3), 21.6 (Ar CH_3), 28.4 ($C(CH_3)_3$), 31.5 (C3′), 49.4 (C5′), 51.4 (C4′), 54.5 (C2′), 70.3 (CH_2OSO_2), 80.9 ($C(CH_3)_3$), 112.3 (C5), 127.8 and 130.1 (Ar CH), 132.7 (Ar CCH_3), 135.7 (C6), 145.3 (Ar CSO_2), 150.9 (C2), 153.5 (Boc CO), 163.1 (C4); *m*/*z* (FAB^+) 612 ($[M + Cs]^+$, 27%), 394 (100), 345 (43), 312 (47), 286 (90); HRMS *m*/*z* (FAB^+) 612.0792 ($[M + Cs]^+$, $C_{22}H_{29}N_3O_7SCs$ requires *m*/*z,* 612.0781).

***N*-(*tert*-Butoxycarbonyl)-(2′*R*,4′*R*)-6,2′-imino(methyl)-4′-(thymin-1-yl)pyrrolidine (18).** Lithium azide (45 mg, 0.93 mmol) was added to a solution of tosyl derivative **15** (111 mg, 0.23 mmol) in dry DMF (1 mL) and the mixture was stirred at 80 °C for 16 h. The solution was allowed to cool to room temperature whereupon saturated brine (10 mL) was added. The mixture was extracted with ethyl acetate (4 × 10 mL), dried over anhydrous $MgSO_4$, filtered and evaporated under reduced pressure. Purification by column chromatography (10% CH_3OH in CH_2Cl_2) gave the enamine **18** (38 mg, 72% based on unrecovered starting material) as a white crystalline solid. R_f 0.31 (10% CH_3OH in CH_2Cl_2); δ_H (300 MHz, $CDCl_3$) 1.47 and 1.49 (total 9H, 2 × s, $C(CH_3)_3$ rotamers), 1.76 (1H, d, *J* 13.6, H_a3'), 1.90 (3H, s, thymine CH_3), 2.26–2.48 (1H, m, H_b3'), 3.03 (1H, t, *J* 13.2, $NHCH_aH_b$), 3.46 (1H, t, *J* 12.4, H_a5'), 3.62–3.87 (2H, m, H_b5' and $NHCH_aH_b$), 4.20–4.42 (1H, m, H2′ rotamers), 5.96 (1H, t, *J* 7.4, H4′), 9.37 (1H, br s, NH); δ_C (100.6 MHz, $CDCl_3$) 9.4 (thymine CH_3), 28.8 ($C(CH_3)_3$), 37.7 and 38.3 (C3′ rotamers), 50.0 and 50.9 ($NHCH_2$ rotamers), 51.6 and 51.9 (C5′ rotamers), 53.1 and 54.1 (C4′ rotamers), 54.2 and 54.6 (C2′ rotamers), 80.5 ($C(CH_3)_3$), 91.3 and 91.6 (C5 rotamers), 151.2 (C2), 153.6 and 153.9 (C6 rotamers), 154.3 and 154.5 (Boc CO rotamers), 163.2 (C4); *m*/*z* (FAB^+) 345 ($[M + Na]^+$, 17%), 323 ($[M + H]^+$, 100), 267 (92); HRMS *m*/*z* (FAB^+) 323.1702 ($[M + H]^+$, $C_{15}H_{23}N_4O_4$ requires *m*/*z,* 323.1719).

***N*-(*tert*-Butoxycarbonyl)-(2′*R*,4′*R*)-2′-[(phthalimido)methyl]-4′-(thymin-1-yl)pyrrolidine 13.** PPh_3 (833 mg, 3.18 mmol) and phthalimide (470 mg, 3.18 mmol) were added to a solution of alcohol **12** (794 mg, 2.44 mmol) in dry THF (20 mL). The mixture was stirred at −15 °C and DEAD (500 μL, 3.18 mmol) was added dropwise over 20 min. After a further 30 min the reaction was warmed to room temperature and stirred for 18 h. Evaporation under reduced pressure and subsequent purification by column chromatography (ethyl acetate) gave the phthalimide derivative **13** (690 mg, 63%) as a white solid. R_f 0.3 (ethyl acetate); mp 102–105 °C (from hexane–ethyl acetate); $[\alpha]_D$ −54.0 (*c* = 1.56, CH_2Cl_2); ν_{max} ($CHCl_3$)/cm^{-1} 3686, 3396, 1774 (Phth CO), 1718 and 1692 (CO); δ_H (270 MHz, $CDCl_3$) 1.33 (9H, br s, $C(CH_3)_3$), 1.96 (3H, d, *J* 0.6, thymine CH_3), 1.92–2.05 (1H, m, H_a3'), 2.43–2.51 (1H, m, H_b3'), 3.41 (1H, dd, *J* 11.9, 7.4, H_a5'), 3.71–3.77 (1H, m, H_b5'), 3.88–4.09 (2H, m, Phth-CH_2), 4.22–4.42 (1H, m, H2′), 4.93–4.99 (1H, m, H4′), 7.28 (1H, s, H6), 7.66–7.74 (2H, m, Ar), 7.79–7.86 (2H, m, Ar), 9.26 (1H, s, NH); δ_C (67.9 MHz, $CDCl_3$) 12.4 (thymine CH_3), 28.2 and 28.3 ($C(CH_3)_3$ rotamers), 33.9 (C3′), 41.6 (Phth-CH_2), 48.5 and 48.6 (C5′ rotamers), 53.4 (C4′), 54.4 (C2′), 80.8 ($C(CH_3)_3$), 111.6 (C5), 123.3 and 134.0 (ArCH), 132.1 (ArC *ipso*), 136.4 (C6), 150.9 (C2), 154.4 (Boc CO), 163.5 (C4), 168.4 (Phth CO); *m*/*z* (FAB^+) 477 ($[M + Na]^+$, 5%), 455 ($[M + H]^+$, 8), 400 (7), 355(100); HRMS *m*/*z* (FAB^+) 455.1924 ($[M + H]^+$, $C_{23}H_{27}N_4O_6$ requires *m*/*z,* 455.1931).

***N*-(*tert*-Butoxycarbonyl)-(2′*R*,4′*R*)-2′-[(amino)methyl]-4′-(thymin-1-yl)pyrrolidine (14).** A solution of phthalimide derivative **13** (340 mg, 0.88 mmol) in a 25–30% aqueous solution of methylamine (2 mL) was heated at 40 °C for 1 h. Evaporation under reduced pressure followed by column chromatography (20% CH_3OH in CH_2Cl_2) gave the amine **14** (253 mg, 89%) as a white solid. R_f 0.28 (30% CH_3OH in CH_2Cl_2); mp 116–118 °C (from CH_3OH–CH_2Cl_2); $[\alpha]_D$ +22.1 (*c* = 0.54, CH_3OH); ν_{max} ($CHCl_3$)/cm^{-1} 3680, 3390, 3020, 1690 (CO), 1470; δ_H (270 MHz, CD_3OD) 1.47 (9H, s, $C(CH_3)_3$), 1.89 (3H, d, *J* 1.1, thymine CH_3), 2.09–2.23 (1H, m, H_a3'), 2.33–2.46 (1H, m, H_b3'), 2.94 (2H, d, *J* 4.9, CH_2NH_2), 3.26–3.37 (1H, m, H_a5'), 3.81–4.00 (2H, m, H_b5' and CH2′), 4.68–4.92 (1H, m, CH4′), 7.57 (1H, d, *J* 1.1, H6); δ_C (67.9 MHz, CD_3OD) 12.3 (thymine CH_3), 28.7 ($C(CH_3)_3$), 33.7 (C3′), 45.3 (CH_2NH_2), 50.1 (C5′), 54.4 (C4′), 59.1 (C2′), 81.7 ($C(CH_3)_3$), 111.8 (C5), 139.5 (C6), 153.0 (C2), 156.4 (Boc CO), 166.3 (C4); *m*/*z* (FAB^+) 455 ($[M + Cs]^+$, 13%), 347 ($[M + Na]^+$, 20), 325 ($[M + H]^+$, 100), 225 (96), 175 (43);

HRMS *m/z* (FAB$^+$) 325.1864 ([M + H]$^+$, $C_{15}H_{25}N_4O_4$ requires *m/z,* 325.1876).

(2′*R*,4′*R*)-2′-[(Phthalimido)methyl]-4′-(thymin-1-yl)pyrrolidine trifluoroacetic acid salt (19). CF_3CO_2H (2.0 mL) was added to a solution of phthalimide derivative **13** (830 mg, 1.83 mmol) in dichloromethane (4.0 mL). After stirring at room temperature for 4 h the solution was reduced in volume under a stream of argon to give a thick oil. On addition of diethyl ether (5.0 mL) and cooling to 0 °C, a precipitate formed which was filtered and dried to give the desired amine salt **19** (740 mg, 86%) as a white solid. $[\alpha]_D$ −46.3 (*c* = 0.19, 10% CH_3OH in CH_2Cl_2); λ_{max} (EtOH)/nm 219 (ε/dm^3 mol^{-1} cm^{-1} 45050); δ_H (400 MHz, DMSO-d6) 1.79 (3H, s, thymine CH_3), 1.99–2.03 (1H, m, H_a3′), 2.54–2.64 (1H, m, H_b3′), 3.37–3.59 (2H, m, H5′), 3.80–3.86 (1H, m, H2′), 3.93–4.04 (2H, m, Phth-CH_2), 5.14–5.22 (1H, br m, H4′), 7.66 (1H, d, *J* 1.0, H6), 7.85–7.95 (4H, m, Ar), 8.90 and 9.80 (each 1H, br s, NH1′), 11.42 (1H, s, thymine NH); δ_C (100.6 MHz, DMSO-d6) 12.1 (thymine CH_3), 32.9 (C3′), 37.7 (C5′), 48.0 (Phth-*C*H_2), 53.6 (C4′), 58.2 (C2′), 109.7 (C5), 117.1 (q, *J* 299.2, CF_3), 123.2, 131.7 and 134.5 (3 × Ar), 138.6 (C6), 151.2 (C2), 158.4 (q, *J* 31.3, CF_3*C*O), 163.7 (C4), 167.9 (Phth CO); *m/z* (FAB$^+$) 355 (M$^+$, 100%), 307 (12), 176 (14); HRMS *m/z* (FAB$^+$) 355.1393 (M$^+$, $C_{18}H_{19}N_4O_4$ requires *m/z,* 355.1406).

***N*-(*tert*-Butoxycarbonyl)-(2′*R*,4′*R*)-2′-[(bromoacetamido)methyl]-4′-(thymin-1-yl)pyrrolidine (20).** To a 65% (w/v) solution of bromoacetic anhydride (13 μL, 0.031 mmol) in acetonitrile was added dichloromethane (500 μL). This was cooled to −8 °C and a solution of amine **14** (10 mg, 0.031 mmol) in dichloromethane (1 mL) was added. After 5 min, the flask was warmed to room temperature and evaporated under reduced pressure. Column chromatography (5⟶10% CH_3OH in CH_2Cl_2) gave the bromoacetamide **17** (13.4 mg, 97%) as a white solid. R_f 0.29 (5% CH_3OH in CH_2Cl_2); mp 90–92 °C (from CH_3OH–CH_2Cl_2); $[\alpha]_D$ −38.1 (*c* = 0.16, CH_3OH); λ_{max} (EtOH)/nm 270.7 (ε/dm^3 mol^{-1} cm^{-1} 20852); δ_H (400 MHz, CD_3OD) 1.49 (9H, s, C(CH_3)$_3$), 1.88 (3H, d, *J* 1.1, thymine CH_3), 2.04–2.22 (1H, m, H_a3′), 2.34–2.48 (1H, m, H_b3′), 3.27–3.41 (1H, m, H_a5′), 3.53–3.64 (2H, m, CH_2Br), 3.87 (2H, d, *J* 2.4, NHCH_2), 3.88–4.12 (2H, m, H_b5′ and H2′), 4.72–4.96 (1H, m, H4′), 7.45 (1H, d, *J* 1.1, H6); δ_C (67.9 MHz, CD_3OD) 12.5 (thymine CH_3), 28.7 (C(CH_3)$_3$), 29.1 (CH_2Br), 33.4 (C3′), 43.3 (CH_2NH), 50.0 C(5′), 54.7 (C4′), 57.1 (C2′), 81.8 and 81.9 (*C*(CH_3)$_3$ rotamers), 111.7 (C5), 139.4 and 139.5 (C6 rotamers), 152.8 (C2), 156.2 (Boc CO), 166.2 (C4), 170.1 (BrCH_2*C*O); *m/z* (FAB$^+$) 469 ([M + Na]$^+$, 5%)‡, 467 ([M + Na]$^+$, 4)§, 447 ([M + H]$^+$, 10)‡, 445 ([M + H]$^+$, 10)§, 347 (100), 345 (98), 314 (84); HRMS *m/z* (FAB$^+$) 445.1090 ([M + H]$^+$, $C_{17}H_{26}N_4O_5{}^{79}$Br requires *m/z,* 445.1087).

Phth-T_2-Boc-POM (21)

Triethylamine (24 μL, 0.172 mmol) was added to a solution of amine **19** (20 mg, 0.043 mmol) and bromoacetamide **20** (19 mg, 0.043 mmol) in dry DMF (0.5 mL). This mixture was stirred at room temperature for 16 h, then evaporated under reduced pressure. A 10% (w/v) K_2CO_3 solution in saturated brine (5 mL) was added and the mixture was extracted with ethyl acetate (4 × 5 ml). The combined extracts were dried over anhydrous $MgSO_4$, filtered and evaporated under reduced pressure. Column chromatography (10% CH_3OH in CH_2Cl_2) gave hydroxyacetamide **23** (8 mg, 49%) and Phth-T_2-Boc-POM **21** (15 mg, 49%) as a white crystalline solid. R_f 0.46 (10% CH_3OH in CH_2Cl_2); mp 122–125 °C (from CH_3OH–CH_2Cl_2); $[\alpha]_D$ −70.83 (*c* = 0.12, CH_3OH); ν_{max} ($CHCl_3$)/cm^{-1} 3690, 3410, 3024, 1780 (Phth CO), 1700 (CO); δ_H (400 MHz, CD_3OD) 1.37 (9H, s, C(CH_3)$_3$), 1.71 and 1.75 (both 3H, s, thymine CH_3), 1.83–1.93 (1H, m, H_a3′), 2.09–2.25 (1H, m, H_b3′), 2.36–2.46 (2H, m, H3′), 2.60 (1H, dd, *J* 11.1, 6.1, H5′), 2.86–2.94 (2H, m, 2 × H2′), 3.19–3.27 (1H, m, H5′), 3.33 (1H, t, *J* 9.9, H5′), 3.47–3.54 (2H, m, CH_2CONH), 3.71 (1H, dd, *J* 14.4, 2.3, Phth-CH_aH$_b$), 3.81 (1H, dd, *J* 14.6, 4.8, Phth-CH$_a$$H_b$), 3.85 (1H, dd, *J* 10.6, 3.5, CONHCH_aH$_b$), 3.89 (1H, s, H5′), 3.92–3.99 (1H, m, CONHCH$_a$$H_b$), 4.59–4.66 and 4.69–4.74 (each 1H, m, H4′), 7.45 (1H, s, H6), 7.67 (4H, br, Ar), 7.70 (1H, s, H6); δ_C (100.6 MHz, CD_3OD) 12.9 (2 × thymine CH_3, coincident), 29.2 (C(*C*H_3)$_3$), 34.2 and 37.6 (2 × C3′), 40.3 (Phth-CH_2), 43.3 (*C*H_2CONH), 50.0 (C5′), 55.5 (C2′), 57.6 (C4′), 57.9 (C5′), 59.1 (C4′), 64.0 (C2′), 82.1 (*C*(CH_3)$_3$), 111.4 and 112.0 (2 × C5), 124.7, 133.5 and 136.1 (Ar), 140.3 and 140.6 (2 × C6), 153.2 and 153.3 (2 × C2), 156.8 (Boc CO), 166.5 and 166.6 (2 × C4), 170.8 (Phth CO), 173.8 (CH_2*C*ONH); *m/z* (FAB$^+$) 741 ([M + Na]$^+$, 9%), 447 ([M + H]$^+$, 10), 719 ([M + H]$^+$, 100), 619 (24), 460 (86); HRMS *m/z* (FAB$^+$) 719.3176 ([M + H]$^+$, $C_{35}H_{43}N_8O_9$ requires *m/z,* 719.3153).

***N*-*tert*-Butoxycarbonyl-(2′*R*,4′*R*)-2′-[(hydroxyacetamido)methyl]-4′-(thymin-1-yl)pyrrolidine (23).** δ_H (400 MHz, CD_3OD) 1.40 (9H, s, C(CH_3)$_3$), 1.80 (3H, d, *J* 1.3, thymine CH_3), 1.95–2.09 (1H, m, H_a3′), 2.28–2.39 (1H, m, H_b3′), 3.26–3.32 (1H, m, H_a5′), 3.48 (2H, br s, NHCH_2), 3.86 (1H, dd, *J* 10.9, 8.1, H_b5′), 3.90 (2H, s, CH_2OH), 3.93–3.98 (1H, m, H2′), 4.72 (1H, m, H4′), 7.39 (1H, d, *J* 1.0, H6), 8.07 (1H, br s, CH_2CON*H*); δ_C (100.6 MHz, CD_3OD) 12.8 (thymine CH_3), 29.1 (C(*C*H_3)$_3$), 34.1 (C3′), 43.4 (C5′), 43.6 (Phth-CH_2), 55.2 (C4′), 57.4 (C2′), 63.1 (CH_2OH), 82.3 (*C*(CH_3)$_3$), 112.2 (C5), 139.9 (C6), 153.3 (C2), 156.8 (Boc CO), 166.7 (C4), 176.1 and 176.1 (CH_2*C*ONH rotamers); *m/z* (FAB$^+$) 383 ([M + H]$^+$, 12%), 283 (100); HRMS *m/z* (CI) 383.1934 ([M + H]$^+$, $C_{17}H_{27}N_4O_6$ requires *m/z,* 383.1930).

Phth-T_2-Boc-POM (21) *via* optimised *N*-alkylation. DIPEA (0.33 mL, 1.89 mmol) was added to a solution of amine **19** (300 mg, 0.63 mmol) and bromoacetamide **20** (280 mg, 0.63 mmol) in dry DMF (2 mL) and the mixture stirred under argon at room temperature for 18 h. Evaporation under reduced pressure gave a residue to which was added brine (10 mL). The mixture was extracted with CH_2Cl_2 (4 × 10 mL), dried over anhydrous $MgSO_4$, filtered, evaporated and then purified by column chromatography (10% CH_3OH in CH_2Cl_2) to give Phth-T_2-Boc-POM **21** (440 mg, 98%) as a white crystalline solid.

Phth-T_2-Boc-POM (21) *via* *N*-acylation. Amine **14** (18 mg, 0.056 mmol) was added to a solution of pentafluorophenyl ester **26** *vide infra* (32 mg, 0.056 mmol) in CH_2Cl_2 (2 mL) and the mixture stirred at room temperature for 3 h. Evaporation under reduced pressure and purification by column chromatography (5⟶10% CH_3OH in CH_2Cl_2) gave Phth-T_2-Boc-POM **21** (40 mg, 100%) as a white crystalline solid.

(2′*R*,4′*R*)-*N*-[(*tert*-Butoxycarbonyl)methyl]-2′-[(phthalimido)methyl]-4′-(thymin-1-yl)pyrrolidine (24). DIPEA (74 μL, 0.428 mmol) and then *tert*-butyl bromoacetate (35 μL, 0.214 mmol) was added to a solution of amine **19** (50 mg, 0.141 mmol) in dry DMF (0.5 mL) at 0 °C. After 5 min the reaction was warmed to room temperature and stirred for a further 18 h. Evaporation under reduced pressure followed by column chromatography (10% CH_3OH in CH_2Cl_2) gave the ester **24** (46 mg, 92%) as a white powder, mp 80–82 °C (from CH_3OH–CH_2Cl_2); $[\alpha]_D$ −9.56 (*c* = 0.46, CH_2Cl_2); ν_{max} ($CHCl_3$)/cm^{-1} 3690, 1770 (Pht CO), 1734, 1715, 1698 and 1684 (C=O); δ_H (300 MHz, $CDCl_3$) 1.34 (3H, s, thymine CH_3), 1.42 (9H, s, C(CH_3)$_3$), 1.80–1.93 (1H, m, H_a3′), 2.43–2.57 (1H, m, H_b3′), 2.61–2.73 (1H, m, H_a5′), 2.90–2.96 (1H, m, H2′), 3.01 (1H, d, *J* 17.0, CH_aH$_b$CO$_2$^{t}Bu), 3.29 (1H, d, *J* 10.4, H_b5′), 3.72–3.79 (2H, m,

‡ As a consequence of ^{81}Br.
§ As a consequence of ^{79}Br.

Phth-CH_2), 3.83 (1H, d, *J* 17.0, $CH_aH_bCO_2{}^tBu$), 4.78–4.88 (1H, m, H4′), 7.62–7.70 and 7.71–7.79 (each 2H, m, Ar), 7.81 (1H, s, H6), 8.97 (1H, s, thymine NH); δ_C (67.9 MHz, $CDCl_3$) 12.0 (thymine CH_3), 28.1 ($C(CH_3)_3$), 37.0 (C3′), 39.0 (Phth-CH_2), 52.4 (C4′), 54.0 ($CH_2CO_2{}^tBu$), 57.8 (C5′), 61.2 (C2′), 81.3 ($C(CH_3)_3$), 110.6 (C5), 123.3, 131.8 and 134.2 (3 × Ar), 137.9 (C6), 150.9 (C2), 163.5 (C4), 168.4 (Phth CO) and 169.6 ($CO_2{}^tBu$); *m/z* (FAB^+) 469 ([M + H]$^+$, 25%), 413 (44), 314 (100), 254 (85); HRMS *m/z* (FAB^+) 469.2103 ([M + H]$^+$, $C_{24}H_{29}N_4O_6$ requires *m/z,* 469.2087).

***N*-Carboxymethyl-(2′*R*,4′*R*)-2′-[(phthalimido)methyl]-4′-(thymin-1-yl)pyrrolidine trifluoroacetic acid salt (25).** Trifluoroacetic acid (0.5 mL) was added to a solution of *tert*-butyl ester **24** (72 mg, 0.154 mmol) in dichloromethane (2.0 mL) and the mixture was stirred for 3 h at room temperature. Evaporation under reduced pressure followed by column chromatography (5⟶15% CH_3OH in CH_2Cl_2) gave the acid **25** (81 mg, 100%) as a white foam. R_f 0.62 (20% CH_3OH in CH_2Cl_2); $[a]_D$ −9.0 (*c* = 0.5, CH_3OH); δ_H (300 MHz, CD_3OD) 1.90–2.10 (1H, m, H_a3'), 2.42–2.55 (1H, m, H_b3'), 2.60–2.76 (1H, m, H_a5'), 2.93–3.15 (1H, m, H2′), 3.04 (1H, d, *J* 17.0, $CH_aH_bCO_2H$), 3.50–3.60 (1H, m, H_b5'), 3.65–3.75 (1H, m, Phth-CH_aH_b), 3.85 (1H, dd, *J* 14.7, 4.9, Phth-CH_aH_b), 3.96 (1H, d, *J* 17.0, CH_aH_b-CO_2H), 4.48–4.57 (1H, m, H4′), 7.67 (4H, s, Ar), 7.95 (1H, s, H6); δ_C (75.5 MHz, CD_3OD) 12.5 (thymine CH_3), 37.6 (C3′), 39.6 (Phth-CH_2), 56.0 (CH_2CO_2H), 56.2 (C4′), 58.5 (C5′), 63.6 (C2′), 111.2 (C5), 117.0 (q, *J* 244.1, CF_3), 124.6, 133.6 and 135.9 (Ar), 141.5 (C6), 153.4 (C2), 163.1 (q, *J* 88.6, CF_3CO_2), 166.6 (C4), 170.6 (Phth CO), 176.7 (CO_2H); *m/z* (FAB^+) 545 ([M + Cs]$^+$, 6%), 435 ([M + Na]$^+$, 10), 423 ([M + H]$^+$, 24), 392 (20), 344 (100); HRMS *m/z* (FAB^+) 413.1443 ([M + H]$^+$, $C_{20}H_{21}N_4O_6$ requires *m/z,* 413.1461).

***N*-(Pentafluorophenoxycarbonyl)methyl-(2′*R*,4′*R*)-2′-[(phthalimido)methyl]-4′-(thymin-1-yl)pyrrolidine (26).** Dry pyridine (5 μL, 0.063 mmol) and pentafluorophenyl trifluoroacetate (6 μL, 0.035 mmol) were added to a solution of acid **25** (15 mg, 0.029 mmol) in dry DMF (100 μL). The mixture was stirred at room temperature for 2 h and then evaporated under reduced pressure. Ethyl acetate (2 mL) and 5% aqueous $NaHCO_3$ (2 mL) were then added and the mixture was extracted with ethyl acetate (5 × 1 mL). The extracts were dried over anhydrous $MgSO_4$, filtered, evaporated under reduced pressure and then purified by column chromatography (ethyl acetate) to give the ester **26** (13 mg, 78%) as a white foam. δ_H (300 MHz, $CDCl_3$) 1.17 (3H, s, thymine CH_3), 1.88–1.99 (1H, m, H_a3'), 2.54–2.68 (1H, m, H_b3'), 2.77 (1H, dd, *J* 11.3, 6.8, H_a5'), 3.00–3.09 (1H, m, H2′), 3.30 (1H, d, *J* 10.9, H_b5'), 3.52 (1H, d, *J* 17.7, $NCH_aH_bCO_2$), 3.80 (1H, dd, *J* 14.7, 1.9, Phth-CH_aH_b), 3.90 (1H, dd, *J* 14.7, 4.5, Phth-CH_aH_b), 4.43 (1H, d, *J* 17.7, $NCH_aH_bCO_2$), 4.83–4.92 (1H, m, H4′), 7.61 (1H, d, *J* 1.14, H6), 7.68 (2H, dd, *J* 5.6, 3.03, Ar), 7.77 (2H, dd, *J* 5.5, 3.03, Ar), 7.95 (1H, s, thymine NH); δ_F (188.2 MHz, $CDCl_3$) −84.04 (2F, dd, *J* 21.8, 17.3, *m*-F), −79.47 (1F, t, *J* 21.8, *p*-F), −74.45 (2F, d, *J* 17.3, *o*-F); *m/z* (FAB^+) 579 ([M + H]$^+$, 100%), 292 (73); HRMS *m/z* (EI) 578.1217 (M^+, $C_{26}H_{19}N_4O_6F_5$ requires *m/z,* 578.1225).

(7*R*,8a*R*)-7-(Thymin-1′-yl)hexahydropyrrolo[1,2-*a*]pyrazin-3-one (28). A solution of Phth-T_2-Boc-POM **21** (71 mg, 0.099 mmol) in 40% (w/v) aqueous methylamine (1 mL) was warmed to 50 °C for 5 h. On cooling to room temperature the solution was evaporated under reduced pressure and purified by column chromatography (10⟶15% CH_3OH in CH_2Cl_2) to give the lactam **28** (18 mg, 69%) as a white foam. δ_H (300 MHz, $CDCl_3$) 1.33–1.44 (1H, m, H_a3'), 1.89 (3H, d, *J* 1.1, thymine CH_3), 2.40–2.68 (3H, m, H_b3', H2′ and H_a5'), 2.86 (1H, d, *J* 16.2, NCH_aH_bCO), 3.03 (1H, d, *J* 11.3, H_b5'), 3.23 (1H, dd, *J* 10.6 and 10.9, $NHCH_aH_b$), 3.38–3.47 (1H, m, $NHCH_aH_b$), 3.65 (1H, d, *J* 16.2, NCH_aH_bCO), 5.30 (1H, m, H4′), 6.78 (1H, br s, CH_2CONH), 7.48 (1H, d, *J* 1.5, H6); δ_C (75.5 MHz, $CDCl_3$) 13.1 (thymine CH_3), 37.0 (C3′), 46.8 ($NHCH_2$), 52.5 (C4′), 56.4 (NCH_2), 59.1 (C2′), 60.3 (C5′), 112.7 (C5), 137.1 (C6), 151.4 (C2), 164.2 (C4), 169.5 (CH_2CONH); *m/z* (FAB^+) 265 ([M + H]$^+$, 100%), 176 (20); HRMS *m/z* (EI) 264.1225 (M^+, $C_{12}H_{16}N_4O_3$ requires *m/z,* 264.1222).

T_2-Boc-POM (27)

A solution of Phth-T_2-Boc-POM **21** (83 mg, 0.116 mmol) in 40% aqueous methylamine (1 mL) was stirred at room temperature for 40 min. Evaporation under reduced pressure then column chromatography (10⟶15% CH_3OH in $CH_2Cl_2$with 0.5% DIPEA) separated the desired amine **27** at lower R_f from the intermediate product at higher R_f (assumed to be **29**). The latter **29** was treated with 40% aqueous methylamine (1 mL) for a further 30 min; evaporation and purification as before gave H_2N-T_2-Boc-POM **27** as a white foam (combined yield of 51 mg, 75%). δ_H (300 MHz, CD_3OD) 1.50 (9H, br s, $C(CH_3)_3$), 1.90 and 1.91 (each 3H, s, thymine CH_3), 2.27–2.65 (4H, m), 2.73–2.94 (2H, m), 2.94–3.18 (3H, m), 3.19–3.34 (1H, m), 3.44–3.79 (4H, m), 3.85–4.15 (2H, m), 4.63–4.82 and 4.96–5.11 (each 1H, m, H4′), 7.48 and 7.83 (each 1H, s, H6); δ_C (75 MHz, CD_3OD) 12.7 and 12.9 (2 × thymine CH_3), 24.4 (C3′), 29.1 ($C(CH_3)_3$), 33.5, 36.3, 41.6, 43.5, 45.4, 54.4, 57.6, 57.8, 60.0, 64.2 (2 × C1′, 2 × C2′, C3′, 2 × C4′, 2 × C5′ and NCH_2CONH), 82.2 and 82.5 ($C(CH_3)_3$ rotamers), 112.0 and 112.4 (2 × C5), 140.1 and 140.4 (2 × C6), 153.2 and 153.3 (2 × C2), 166.8 and 166.8 (2 × C4), 174.2 (CH_2CONH); *m/z* (FAB^+) 627 ([M + K]$^+$, 3%), 511 (5), 345 (60); HRMS *m/z* (FAB^+) 627.2893 ([M + K]$^+$, $C_{27}H_{40}N_8O_7K$ requires *m/z,* 627.2657).

T_2-POM·3HCl (30)

T_2-Boc-POM **27** (51 mg, 0.087 mmol) was dissolved in a solution of 1 : 1 THF–CH_3OH (1 mL) saturated with HCl gas. After stirring for 15 minutes a white precipitate formed. The mixture was then cooled to 0 °C for 10 min and filtered. The filtrate was re-cooled to 0 °C and a second batch of precipitate was collected. The combined precipitate was dried under reduced presure to give T_2-POM hydrochloride salt **30** (49 mg, 94%) as a white solid. δ_H (500 MHz, D_2O) 1.88 (3H, s, thymine CH_3), 2.00 (3H, s, thymine* CH_3), 2.19 (1H, ddd, *J* 14.0, 9.9, 6.2, H3′), 2.26 (1H, ddd, *J* 14.3, 11.5, 6.5, H*3′), 2.77 (1H, ddd, *J* 14.3, 9.6, 7.4, H*3″), 2.93 (1H, ddd, *J* 14.0, 9.6, 7.4, H3″), 3.38 (1H, dd, *J* 13.6, 7.8, H6′), 3.47 (1H, dd, *J* 12.5, 8.8, H5″), 3.51 (2H, dd, *J* 13.6, 3.4, H6″), 3.70 (1H, dd, *J* 13.4, 7.8, H*5″), 3.79 (1H, d, *J* 16.1, H7′), 3.81 (1H, dd, *J* 13.4, 2.8, H*5′), 3.86 (2H, dd, *J* 15.3, 4.1, H*6′ and H*6″), 3.91 (1H, dd, *J* 12.5, 3.7, H5′), 3.93 (1H, dddd, *J* 11.1, 7.4, 41, 4.1, H*2′), 4.11 (1H, d, *J* 16.1, H7″), 4.86 (1H, dddd, *J* 9.6, 7.8, 6.5, 2.8, H*4′), 5.03 (1H, dddd, *J* 9.6, 8.8, 6.2, 3.7, H4′), 7.48 (1H, s, H*6), 7.61 (1H, s, H6). *Denotes lower pyrrolidine ring (see ESI for numbering system). δ_C (100.6 MHz, D_2O) 11.6 and 11.7 (2 × thymine CH_3), 31.6 and 33.4 (2 × C3′), 39.1 and 39.3 (2 × C5′), 49.5, 55.1, 59.3 (2 × C6′, NCH_2CO), 57.1, 60.1, 60.8, 63.3 (2 × C2′, 2 × C4′), 110.8 and 111.5 (2 × C5), 142.1 and 143.5 (2 × C6), 152.3 and 152.7 (2 × C2), 166.8 and 167.0 (2 × C4), 171.5 (CH_2CONH); *m/z* (FAB^+) 511 ([M − 3HCl + Na]$^+$, 98%), 489 ([M − 3HCl + H]$^+$, 100); HRMS *m/z* (FAB^+) 489.2565 ([M − 3HCl + H]$^+$, $C_{22}H_{33}N_8O_5$ requires *m/z,* 489.2574).

Phth-T_3-Boc-POM (32)

Phth-T_2-Boc-POM **21** (370 mg, 0.515 mmol) was added to a 20% solution of CF_3CO_2H in CH_2Cl_2 (10 mL) and stirred at room temperature for 4 h. The solvent was removed under a stream of argon followed by evaporation under reduced pressure. Dry DMF (2 mL), bromoacetamide **20** (229 mg, 0.515 mmol) and DIPEA (450 μL, 2.58 mmol) were then added and

the solution stirred at room temperature for 16 h. Evaporation under reduced pressure and purification by column chromatography (10⟶20% CH_3OH in CH_2Cl_2) gave Phth-T_3-Boc-POM **32** (0.490 g, 97%) as a white solid. R_f 0.27 (9% CH_3OH and 1% Et_3N in CH_2Cl_2); δ_H (300 MHz, CD_3OD) 1.21 (3H, s, thymine CH_3), 1.51 (9H, s, $C(CH_3)_3$), 1.87 and 1.98 (each 3H, s, thymine CH_3), 1.98–3.20 (12H, m), 3.30–4.40 (13H, m), 4.58–4.67, 4.67–4.82 and 4.97–5.08 (each 1H, m, CH4′), 7.51 (1H, s, H6), 7.73–7.79 (4H, m, Ar), 8.07 and 8.09 (each 1H, s, H6); δ_C (75.5 MHz, CD_3OD) 12.5, 12.8 and 13.2 (3 × thymine CH_3), 33.9, 36.5, 37.6, 39.6, 43.4, 43.5, 54.3, 55.2, 55.7, 56.6, 57.5, 57.9, 58.5, 60.2, 63.0, 63.6 and 65.3 (3 × C2′, 3 × C3′, 3 × C4′, 3 × C5′, 2 × $CONHCH_2$, Phth-CH_2 and 2 × NCH_2CONH), 82.2 ($C(CH_3)$), 111.0, 111.8 and 112.0 (3 × C5), 124.7, 133.7, 133.5 and 135.9 (Ar C), 140.8, 141.0 and 141.1 (3 × C6), 153.1, 153.2 and 153.6 (3 × C2), 156.7 (Boc CO), 166.5, 166.7 and 167.2 (3 × C4), 170.5 (Phth CO), 173.6 and 174.2 (2 × CH_2CONH); *m*/*z* (FAB$^+$) 1005 ([M + Na]$^+$, 50%), 983 ([M + H]$^+$, 100), 883 (42), 466 (48); HRMS *m*/*z* (FAB$^+$) 983.4334 ([M + H]$^+$, $C_{47}H_{59}N_{12}O_{12}$ requires *m*/*z*, 983.4375).

Phth-T_4-Boc-POM (33)

Phth-T_3-Boc-POM **32** (410 mg, 0.418 mmol) was added to a 20% solution of CF_3CO_2H in CH_2Cl_2 (10 mL) and the solution stirred at room temperature for 4 h. The solvent was removed under a stream of argon followed by evaporation under reduced pressure. Dry DMF (2 mL), bromoacetamide **20** (185 mg, 0.418 mmol) and then DIPEA (440 μL, 2.53 mmol) were added and the solution stirred at room temperature for 16 h. Evaporation under reduced pressure and then purification by column chromatography (15% CH_3OH in CH_2Cl_2) gave Phth-T_4-Boc-POM **33** (500 mg, 96%) as a white solid. δ_H (400 MHz, CD_3OD) 1.08, 1.76, 1.83 and 1.85 (each 3H, s, thymine CH_3), 1.38 (9H, s, $C(CH_3)_3$), 1.55–1.64 and 1.78–1.82 (each 1H, m, H_a3'), 1.87–1.95 (2H, m, 2 × H_a3'), 1.99–4.0 (30H, 3 × $NHCH_2CH2'$, Phth-CH_2, 4 × H2′, 4 × H_b3', 4 × H5′ and 3 × NCH_2CONH), 4.48–4.54 (1H, m, H_a4'), 4.54–4.68 (1H, m, H_b4'), 4.85–4.93 (1H, m, H_A4'), 4.75–4.85 (probably 1H, H_B4' masked by residual HDO), 7.36, 7.87, 7.92 and 8.00 (each 1H, s, H6), 7.64 and 7.65 (each 2H, s, Ar); δ_C (100.6 MHz, CD_3OD) 12.6, 12.8, 13.3 and 13.3 (4 × thymine CH_3), 29.2 ($C(CH_3)_3$), 33.7, 36.39, 37.4, 37.6, 38.8, 39.5, 54.3, 54.6, 55.2, 55.6, 56.2, 56.6, 56.9, 57.6, 57.8, 58.4, 59.8, 59.9, 63.6, 64.9 and 65.4 (4 × C2′, 4 × C3′, 4 × C4′, 4 × C5′, 3 × $CONHCH_2$, Phth-CH_2 and 3 × NCH_2CONH)¶, 82.15 ($C(CH_3)_3$), 111.0, 111.6, 111.8 and 111.9 (4 × C5), 124.7, 133.5 and 136.0 (3 × Ar), 140.8, 140.9¶ and 141.1 (4 × C6), 153.1, 153.2, 153.3 and 153.6 (4 × C2), 156.7 (Boc CO), 166.4, 166.7, 166.8 and 167.3 (4 × C4), 170.52 (Phth CO), 173.5, 174.1 and 174.2 (3 × CH_2CONH); MS *m*/*z* (ESI$^+$) 1247.4 ([M + H]$^+$, $C_{59}H_{75}N_{16}O_{15}$ requires *m*/*z*, 1247.6).

Phth-T_5-Boc-POM (34)

Phth-T_4-Boc-POM **33** (240 mg, 0.193 mmol) was added to a 30% solution of CF_3CO_2H in CH_2Cl_2 (6 mL) and stirred at room temperature for 4 h. The solvent was removed under a stream of argon followed by evaporation under reduced pressure. Dry DMF (4 mL), bromoacetamide **20** (94 mg, 0.21 mmol) and then DIPEA (235 μL, 1.35 mmol) were added and the solution stirred at room temperature for 16 h. Evaporation under reduced pressure and purification by column chromatography (10⟶20% CH_3OH in CH_2Cl_2 then 10⟶20% CH_3OH in CH_2Cl_2 with 0.5% DIPEA), gave Phth-T_5-Boc-POM **34** (271 mg, *ca.* 91%) as a white solid containing some residual DIPEA–TFA salt. Repeated recrystallisation *via* slow cooling from a warm saturated methanolic solution afforded an analytically pure sample. δ_H (300 MHz, DMSO-d6) 1.32, 1.73 and 1.75 (each 3H, s, 3 × thymine CH_3), 1.77 (6H, s, 2 × thymine CH_3), 1.40 (9H, s, $C(CH_3)_3$), 1.45–1.60 (3H, m, 3 × H_a3'), 1.92–2.08 (2H, m, 2 × H3′), 2.20–3.90 (38H, 4 × $NHCH_2CH2'$, Phth-CH_2, 5 × H2′, 5 × H3′, 5 × H5′ and 4 × NCH_2CONH), 4.60–4.95 (5H, m, 5 × H4′), 7.54–8.05 (13H, 5 × H6, 4 × Ar and 4 × CH_2CONH), 11.05, 11.12,‖ 11.17 and 11.28 (5H, 5 × thymine NH); *m*/*z* (ESI$^+$) 1511.7 ([M + H]$^+$, $C_{71}H_{91}N_{20}O_{18}$ requires *m*/*z*, 1511.7).

Phth-T_5-POM·5HCl (35)

Phth-T_5-Boc-POM **34** (7 mg, 4.6 μmol) was treated with a 1 : 1 CH_3OH–H_2O mixture saturated with HCl gas (2 mL). The reaction was stirred at 40 °C for 5 min and then at room temperature for 2 h. The methanol was then removed under reduced pressure and the remaining water was lyophilised to give the desired Phth-T_5-POM **35** HCl salt (7 mg, 95%) as a white powder. A sample was subsequently lyophilised twice from D_2O for NMR purposes. δ_H (400 MHz, D_2O) 1.57, 1.65, 1.72, 1.75 and 1.78 (total 15H, 5 × thymine CH_3), 2.00–4.40 (43H, 4 × $NHCH_2CH2'$, 1 × Phth-CH_2, 5 × H2′, 5 × H3′, 5 × H5′ and 4 × NCH_2CONH), 4.38–4.67 (5H, m, 5 × H4′), 7.33–7.55 (5H, m, 5 × H6), 7.81 and 7.82 (total 4H, 2 × s, Ar); *m*/*z* (ESI$^+$) 706.3 ([M − 3H − 5Cl]$^{2+}$, $C_{66}H_{84}N_{20}O_{16}$ requires *m*/*z*, 706.3) and 471.2 ([M − 2H − 5Cl]$^{3+}$, $C_{66}H_{85}N_{20}O_{16}$ requires *m*/*z*, 471.2).

UV hybridisation studies

General. A Varian-Cary 1 UV-Visible spectrophotometer equipped with Peltier heating block and six cell transport mechanism was employed. Quartz cuvettes (24 × 5 × 10 mm) fitted with Teflon stoppers were used throughout. Reference cuvettes always contained the same buffer used in the corresponding sample cuvette. Data were analysed using software provided by Varian-Cary. For thermal denaturation experiments, absorbance readings were recorded at 260 nm (unless stated otherwise) with data collection every 0.1 °C and an averaging time of 1 s. Temperature monitoring was *via* a probe placed inside a cuvette containing buffer and adjacent to the sample cuvette in the cell holder. Concentrations of all oligonucleotides are expressed in mol/base and for each of the oligonucleotides the concentration was 42 μM in bases, unless stated otherwise. The concentrations of stock solutions were obtained *via* serial dilution and for polynucleotides and $d(T)_{20}$ these were determined spectrophotometrically at 80 °C using the Beer–Lambert law and the known extinction coefficients of the corresponding nucleotides [ε/dm^3 mol^{-1} cm^{-1} 15000 for dA, 15000 for rA, 7600 for rC, 12160 for rG, 10210 for rU and 8500 for dT]. For Phth-T_5-POM **35**, the extinction coefficient used was 8920 which represents the sum of the extinction coefficients of thymine (ε = 8500) plus 1/5 of the extinction coefficient of phthalimide (ε = 2100) at 260 nm. All stock solutions were stored at −20 °C in between use. All sample vials and pipette tips were sterile and the H_2O used was doubly distilled prior to use. Silicon oil (Sigma) was used to prevent sample evaporation. All polynucleotides were commercially available (Sigma) while the 5-mer Lys-T_5-LysNH_2-PNA (*N*-terminal lysine and *C*-terminal lysine amide) was purchased from PE/Applied Biosystems, Warrington, UK.

Sample preparation. Unless stated otherwise, thermal melt experiments were carried out using equimolar amounts (in bases) of both oligonucleotides taken from aqueous stock solutions and adding 500 μL of double concentrated buffer. Water was then added to give a total volume of 1 mL and the solution then mixed gently using a pipette before adding it to the cuvette. A thin layer of oil was then added and a Teflon stopper was inserted to prevent evaporation.

¶ Probably two signals are coincident.

‖ Two peaks are coincident.

Procedures for thermal denaturation experiments. For thermal denaturation experiments involving Phth-T_5-POM **35** and poly(rA), an equimolar mixture of the two strands (42 μM each in bases) was initially heated at 5 °C min^{-1} from 25–93 °C in order to completely dissociate the strands. After 1 min at 93 °C, the sample was cooled at 0.2 °C min^{-1} to 15 °C and then after a further 1 min the sample was heated at 0.2 °C min^{-1} to 93 °C. For thermal melting experiments involving Phth-T_5-POM **35** and poly(dA), an equimolar mixture of the two strands was incubated at a concentration of 210 μM each (in bases) at 25 °C for at least 48 h. The sample was then diluted with the appropriate buffer to 1 mL to give a concentration of 42 μM each (in bases). After cooling from 25⟶15 °C at 1 °C min^{-1}, the sample was allowed to equilibrate at 15 °C for at least 1 min and then heated and cooled between 15 and 93 °C at 0.2 °C min^{-1}. For thermal melting experiments involving $d(T)_{20}$ or Lys-T_5-LysNH_2-PNA with either poly(rA) or poly(dA), a protocol identical to that used for the Phth-T_5-POM **35**–poly(rA) thermal melting experiments was followed. For all T_m determination, the temperature at the maximum of the first derivative of the slow melting curve was used. All melting experiments were performed at least twice (except where stated otherwise) and the values shown are the average of these readings.

Procedures for continuous variation experiments. In order to determine the stoichiometry for Phth-T_5-POM **35** binding to poly(rA), different mole ratios of the two strands at 10% increments and a total base concentration of 50 μM in 10 mM K_2HPO_4 buffer adjusted to 0.12 M K^+ and pH 7.0, were mixed by pipette and then allowed to anneal for 24 h at 25 °C. The mixtures were then sequentially transferred into a cuvette and the UV spectra recorded between 300 and 220 nm.

Procedures for kinetic experiments. Using the Varian-Cary kinetic software, absorbance changes at 260 nm were monitored with respect to time at 25 °C immediately upon adding and mixing an equimolar amount of either Phth-T_5-POM **35** or Lys-T_5-LysNH_2-PNA to a buffered solution containing either poly(rA) or poly(dA). Experiments involving the hybridisation between Phth-T_5-POM **35** and poly(rA) were conducted using equimolar mixtures of each strand at base concentrations of 42 μM using a cuvette of path length 1.0 cm. Experiments involving the hybridisation between Phth-T_5-POM **35** and poly(dA) were conducted using equimolar mixtures of each strand at base concentrations of either 42 μM or 210 μM (as indicated) and using cuvettes of path length 1.0 cm or 0.2 cm respectively.

SPR hybridisation studies. The SPR measurements were performed using a BIAcore 2000 instrument (Biacore AB, UK). Streptavidin derivatised carboxymethyl dextran sensor chips (SA) were used as obtained from Biacore. Each sensor chip contained four flow cells (2.4 × 0.5 × 0.05 mm) with a probing spot for the SPR signal of *ca.* 0.26 mm^2 for each flow cell. Buffers used were as for UV melting experiments (0.12 M K^+, pH 5.0, 6.0 or 7.0, and 1.2 M K^+, pH 7.0) and were degassed immediately prior to use. Milli-Q grade water was used throughout. All assays were carried out at 25 °C with data points collected every 0.5 s. Absence of stem loops or dimers in the biotinylated mixed sequence oligonucleotides was confirmed using the computer programmes AMPLIFY and GCG respectively. Data were prepared for analysis and presentation by subtracting the average response recorded 20 s prior to injection and adjusting the time of injection to zero. Data from flow cell 1 (underivatised dextran) were subtracted from the corresponding data obtained from the flow cells (2, 3 and 4) that contained biotinylated oligonucleotides, in order to correct for bulk refractive index changes and signal drift. All oligonucleotides were biotinylated at the 5′-end using multi biotin-III-CE phosphoramidite and were purchased from Cruachem, Glasgow, UK.

General procedures for binding studies. Samples were prepared by serial dilution from aqueous stock solutions. All procedures for binding studies were automated as methods using repetitive cycles of sample injection and regeneration. Samples were injected at a flow rate of 20 μL min^{-1} using the KINJECT command from 7 mm plastic vials that were capped with pierceable plastic crimp caps. In order to minimise carryover, samples were injected in order of increasing concentration. For all injections the running buffer was identical to the injection buffer. Regeneration using 10 mM hydrochloric acid (20 μL, 20 μL min^{-1}) was performed between each injection.

Immobilisation of biotinylated oligonucleotides. Onto the second flow cell of a dextran chip containing streptavidin was injected a solution of ssDNA 5′-biotin-$d(A)_{20}$ at 1 μg mL^{-1} in water for 3 min and at 10 μL min^{-1} until 1450 RU were obtained. In a similar manner, flow cell 3 was derivatised with 1400 RU of ssRNA 5′-biotin-$r(A)_{20}$ and flow cell 4 with 1000 RU of ssDNA 5′-biotin-d(AGC TTC AGA GAT CGA TCG GAG AGA GTA CTG). After at least 100 s of buffer wash, 10 μL of 10 mM hydrochloric acid were passed over all the cells.

T_5-POM, T_5-PNA, $d(T)_5$ and $d(T)_{20}$—oligonucleotide binding assays. Serial two-fold dilutions (160–10 μM, 100 μL, 20 μL min^{-1}) of Phth-T_5-POM **35** in 10 mM K_2HPO_4 adjusted to 0.12 M K^+ and pH 7.0, were passed serially over all four flow cells of the sensor chip. The complex was then washed with buffer for 6 min followed by regeneration using 10 mM hydrochloric acid (20 μL, 20 μL min^{-1}). $d(T)_5$ was assayed in an identical manner using the same concentrations. PNA (Lys-T_5-LysNH_2) was assayed in an identical manner except using serial two-fold dilutions of 40–1.25 μM and $d(T)_{20}$ using 5–0.31 μM dilutions. Assays were performed at different ionic strength and pH (as indicated) following an identical protocol.

Acknowledgements

We thank the EPSRC for a studentship to DTH, the Paterson Cancer Research Institute (Manchester), Dr Alan Tucker for assistance with NMR experiments, the EPSRC National Mass Spectrometry Service Centre (Swansea) and the Michael Baber Centre for Mass Spectrometry.

References

1 J. Micklefield, *Curr. Med. Chem.*, 2001, **8**, 1157.
2 J. Kurreck, *Eur. J. Biochem.*, 2003, **270**, 1628.
3 D. A. Braasch and D. R. Corey, *Biochemistry*, 2002, **41**, 4503.
4 A. Dove, *Nat. Biotechnol.*, 2002, **20**, 121.
5 M. Petersen and J. Wengel, *Trends Biotechnol.*, 2003, **21**, 74.
6 D. A. Braasch and D. R. Corey, *Chem. Biol.*, 2001, **8**, 1.
7 P. E. Nielsen, *Curr. Opin. Biotechnol.*, 1999, **10**, 71.
8 P. E. Nielsen, *Curr. Opin. Biotechnol.*, 2001, **12**, 16.
9 C. Carlsson, M. Jonsson, B. Norden, M. T. Dulay, R. N. Zare, J. Noolandi, P. E. Nielsen, L.-P. Tsui and J. Zielenski, *Nature*, 1996, **380**, 207.
10 F. A. Rogers, K. M. Vasquez, M. Egholm and P. M. Glazer, *Proc. Natl. Acad. Sci. USA*, 2002, **99**, 16695.
11 H. Parekh-Olmedo, M. Drury and E. B. Kmeic, *Chem. Biol.*, 2002, **9**, 1073.
12 C. Richert, A. L. Roughton and S. A. Benner, *J. Am. Chem. Soc.*, 1996, **118**, 4518.
13 Z. Huang and S. A. Benner, *J. Org. Chem.*, 2002, **67**, 3996.
14 A. Eschenmoser, *Science*, 1999, **284**, 2118.
15 S. M. Freier and K.-H. Altmann, *Nucleic Acid Res.*, 1997, **25**, 4429.
16 E. T. Kool, *Chem. Rev.*, 1997, **97**, 1473.
17 J. Wengel, *Acc. Chem. Res.*, 1999, **32**, 301.
18 S. K. Singh and J. Wengel, *Chem. Commun.*, 1998, 1247.
19 A. De Mesmaeker, A. Waldner, J. Lebreton, P. Hoffmann, V. Fritsch, R. M. Wolf and S. M. Freier, *Angew. Chem., Int. Ed. Engl.*, 1994, **33**, 226.

20 K. J. Fettes, N. Howard, D. T. Hickman, S. A. Adah, M. R. Player, P. F. Torrence and J. Micklefield, *Chem. Commun.*, 2000, 765.
21 B. Hyrup and P. E. Nielsen, *Bioorg. Med. Chem.*, 1996, **4**, 5.
22 P. E. Nielsen, *Acc. Chem. Res.*, 1999, **32**, 624.
23 E. Uhlmann, A. Peyman, G. Breipohl and D. W. Will, *Angew. Chem., Int. Ed.*, 1998, **37**, 2796.
24 P. M. Reddy and T. C. Bruice, *Bioorg. Med. Chem. Lett.*, 2003, **13**, 1281.
25 D. T. Hickman, P. M. King, M. A. Cooper, J. M. Slater and J. Micklefield, *Chem. Commun.*, 2000, 2251.
26 G. J. M. Koper, R. C. van Duijvenbode, D. D. P. W. Stam, U. Steuerle and M. Borkovec, *Macromolecules*, 2003, **36**, 2500.
27 G. J. M. Koper, M. H. P. van Genderen, C. Elissen-Román, M. W. P. L. Baars, E. W. Meijer and M. Borkovec, *J. Am. Chem. Soc.*, 1997, **119**, 6512.
28 N. Umezawa, M. A. Gelman, M. C. Haigis, R. T. Raines and S. H. Gellman, *J. Am. Chem. Soc.*, 2002, **124**, 368.
29 T. Furuya, S. Fujita, S. Iwanami, A. Takenka and Y. Sasada, *Acta Crystallogr., Sect. C*, 1986, **42**, 1345.
30 C. Altona and M. Sundaralingam, *J. Am. Chem. Soc.*, 1972, **94**, 8205.
31 W. Saenger, *Principles of Nucleic Acid Structure* (Ed. C. R. Cantor), Springer-Verlag, New York, 1984.
32 E. A. Green, R. D. Rosenstein, R. Shiono, D. J. Abraham, B. L. Trus and R. E. Marsh, *Acta Crystallogr., Sect. B*, 1975, **31**, 102.
33 G. Lowe and T. Vilaivan, *J. Chem. Soc., Perkin Trans. 1*, 1997, 539–560.
34 G. Lowe, T. Vilaivan and M. S. Westwell, *Bioorg. Chem.*, 1997, **25**, 321.
35 M. D'Costa, V. Kumar and K. N. Ganesh, *Org. Lett.*, 1999, **1**, 1513.
36 A. Püschl, T. Tedeschi and P. E. Nielsen, *Org. Lett.*, 2000, **2**, 4161.
37 T. Vilaivan, C. Khongdeesameor, P. Harnyuttanakorn, M. S. Westwell and G. Lowe, *Bioorg. Med. Chem. Lett.*, 2000, **10**, 2541.
38 M. D'Costa, V. Kumar and K. N. Ganesh, *Org. Lett.*, 2001, **3**, 1281.
39 V. Kumar, P. S. Pallan, Meena and K. N. Ganesh, *Org. Lett.*, 2001, **3**, 1269.
40 T. Vilaivan and G. Lowe, *J. Am. Chem. Soc.*, 2002, **124**, 9326.
41 J. J. P. Stewart, *J. Comput. Aided Mol. Des.*, 1990, **4**, 1.
42 G. L. Baker, S. J. Fritschel, J. R. Stille and J. K. Stille, *J. Org. Chem.*, 1981, **46**, 2954.
43 T. Sasaki, K. Minamoto, T. Suzuki and T. Sugiura, *J. Am. Chem. Soc.*, 1978, **100**, 2248.
44 T. Sasaki, K. Minamoto, T. Suzuki and T. Sugiura, *J. Org. Chem.*, 1979, **44**, 1424.
45 Z. Dzakula, M. L. DeRider and J. L. Markley, *J. Am. Chem. Soc.*, 1996, **118**, 12796.
46 P. Job, *Ann. Chim.*, 1928, **9**, 113.
47 G. Felsenfeld, *Biochim. Biophys. Acta*, 1958, **29**, 133.
48 R. O. Dempcy, K. A. Browne and T. C. Bruice, *Proc. Natl. Acad. Sci. USA*, 1995, **92**, 6097.
49 R. O. Dempcy, K. A. Browne and T. C. Bruice, *Proc. Natl. Acad. Sci. USA*, 1995, **92**, 7051.
50 M. Wasner, D. Arion, G. Borkow, A. Noronha, A. H. Uddin, M. A. Parniak and M. J. Damha, *Biochemistry*, 1998, **37**, 7478.
51 T. L. Sheppard and R. C. Breslow, *J. Am. Chem. Soc.*, 1996, **118**, 9810.
52 J. S. Pudlo, X. Cao, S. Swaminathan and M. D. Matteucci, *Tetrahedron Lett.*, 1994, **35**, 9315.
53 J. D. McGhee and P. H von Hippel, *J. Mol. Biol.*, 1974, **86**, 469.
54 M. Malmqvist, *Nature*, 1993, **361**, 186.
55 M. Hendrix, S. E. Priestley, G. F. Joyce and C.-H. Wong, *J. Am. Chem. Soc.*, 1997, **119**, 3641.
56 K. K. Jensen, H. Ørum, P. E. Nielsen and B. Nordén, *Biochemistry*, 1997, **36**, 5072.